

Batteries for Transportation

An overview of degradation phenomena that determine the lifetime of lithium ion batteries

Mark Verbrugge
General Motors R&D Center

Outline

- ❑ GM HEV, pHEV, and EREV plans
- ❑ Chemical degradation (better understood)
 - Negative electrode
 - Positive electrode
 - SEI (solid electrolyte interface)
 - Life models
 - Solid mechanics (stress distribution)
- ❑ Summary of combined chemical and mechanical degradation

Global Energy Concerns (for every nation state)

Energy security

Secure

Environmental health

Clean

Economic competitiveness

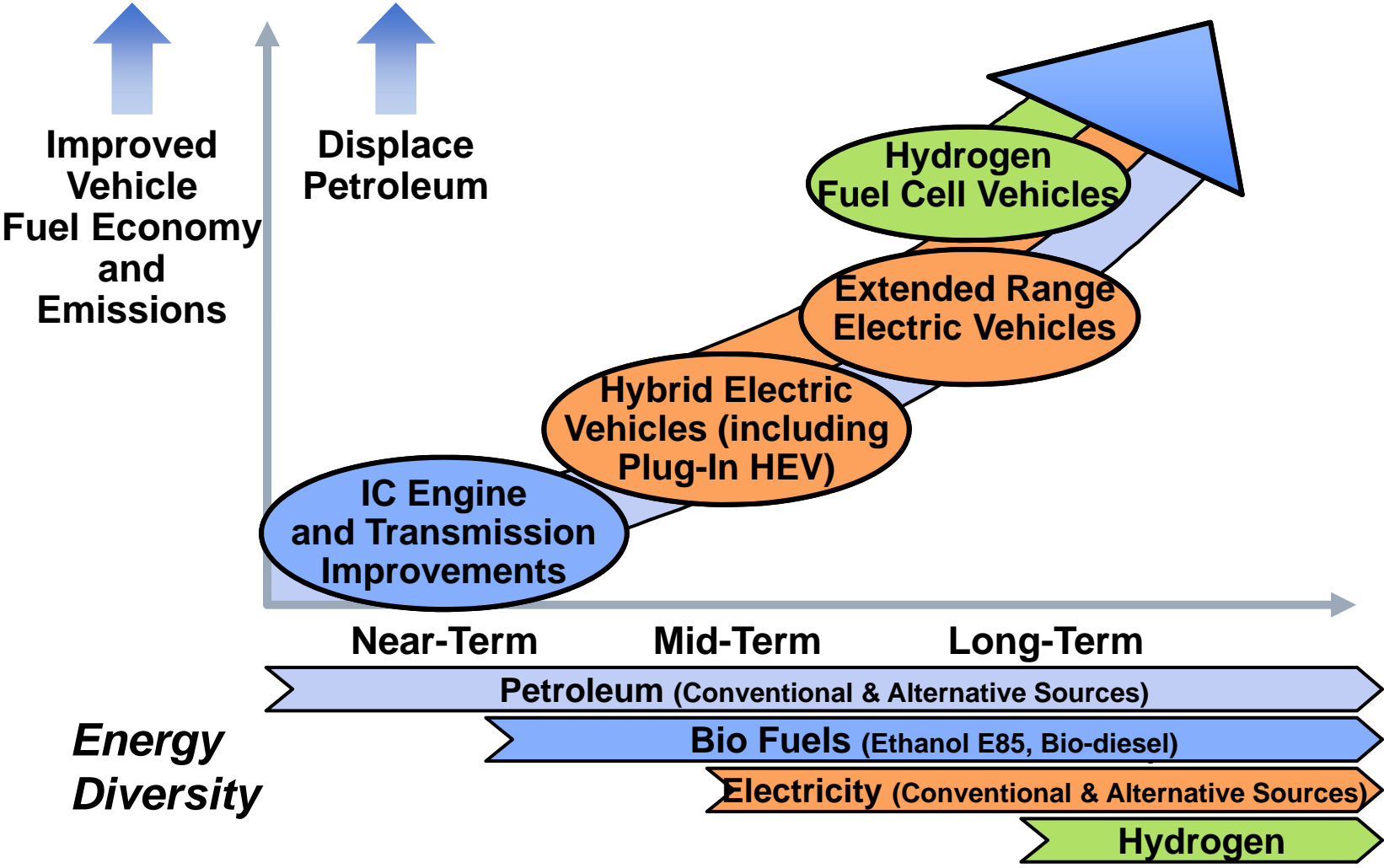
Affordable

Sustainability &
National Security

To some extent, we can reduce demand, but the **ultimate solution will come out of advancements in science and technology.**



Advanced Propulsion Technology Strategy





coskata



MASCOMA














GM Hybrid and Electric Programs

Lithium ion post 2010



GM-Allison Hybrid

	2001	2002	2003	2004	2005	2006	2007	2008	2009	
GM-Allison Hybrid			GM/Allison Hybrid Bus							
GM Hybrid						Saturn VUE Green Line				
						Saturn AURA Green Line Chevrolet Malibu Hybrid				
						Shanghai GM Buick LaCrosse Eco-Hybrid				
RWD 2-Mode Hybrid							Tahoe/Yukon			
							Escalade			
						Silverado/Sierra				
FWD 2-Mode Hybrid							Saturn VUE Green Line 2-Mode			
								VUE PHEV		
E-REV									Volt E-REV	



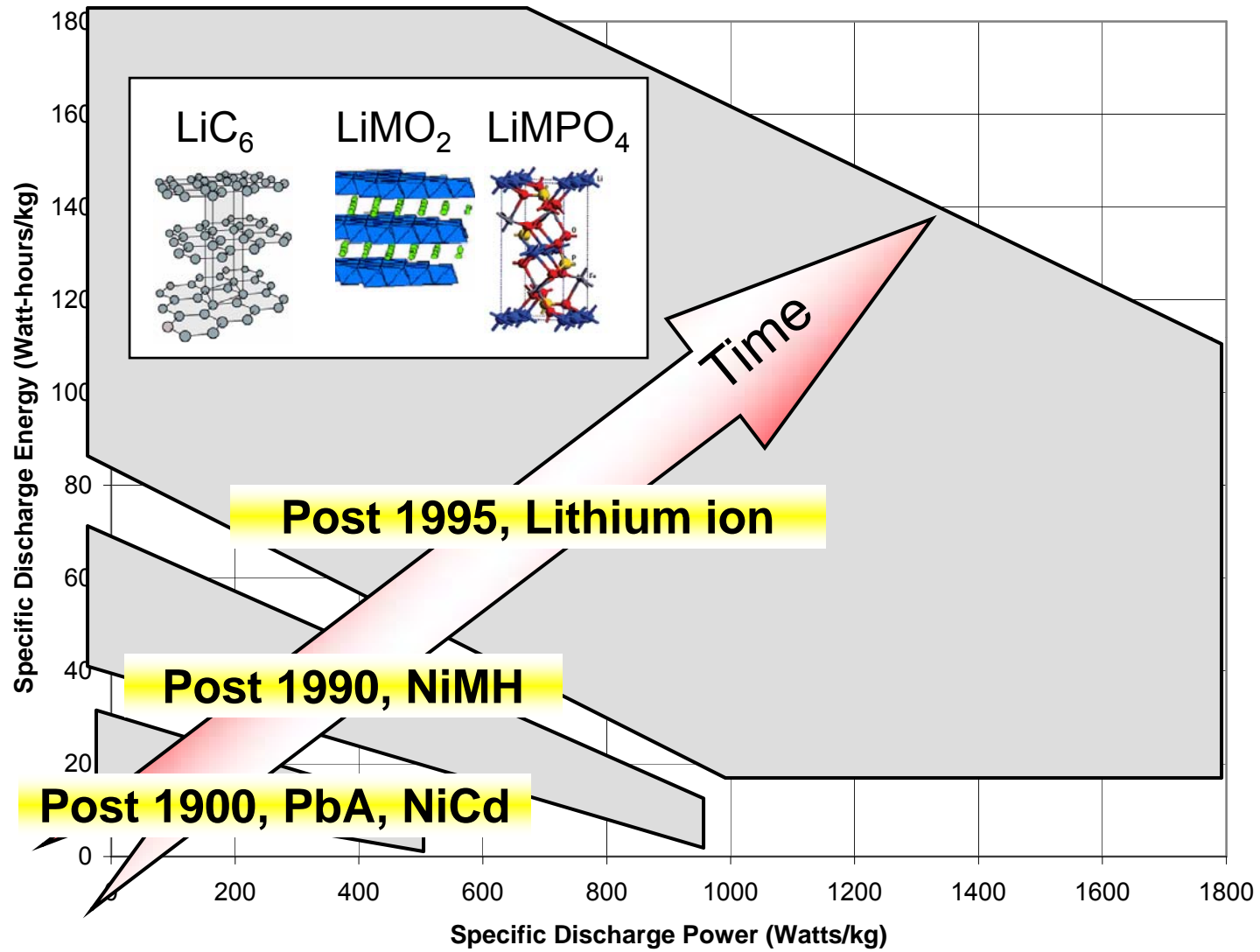
Comparison of GM's requirements to USABC specs



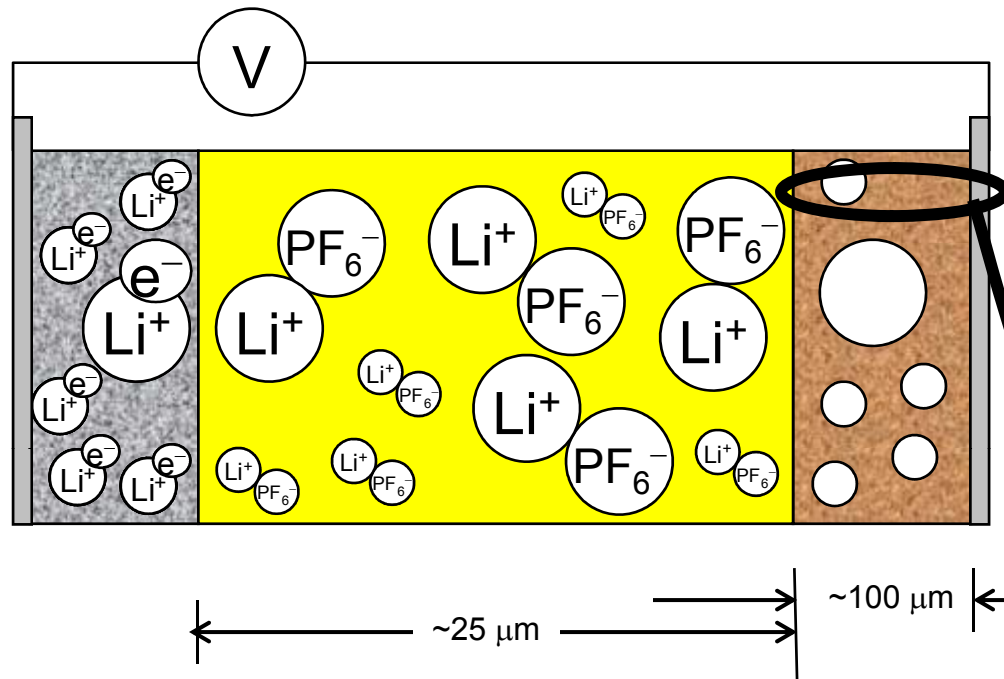
Requirements of End of Life Energy Storage Systems for PHEVs

Characteristics at EOL (End of Life)		High Power/Energy Ratio Battery	GM 2-Mode PHEV	High Energy/Power Ratio Battery	EFLEX EREV
Reference Equivalent Electric Range	miles	10	10	10	10
Peak Pulse Discharge Power - 2 Sec / 10 Sec	kW	50 / 45	50/45	46 / 38	115/110
Peak Regen Pulse Power (10 sec)	kW	30	27	25	60
Available Energy for CD (Charge Depleting) Mode, 10 kW Rate	kWh	3.4	3.5	11.6	8
Available Energy for CS (Charge Sustaining) Mode	kWh	0.5	0.3	0.3	0.35
Minimum Round-trip Energy Efficiency (USABC HEV Cycle)	%	90	90	90	90
Cold cranking power at -30°C, 2 sec - 3 Pulses	kW	7	7	7	8
CD Life / Discharge Throughput	Cycles/MWh	5,000 / 17		5,000 / 58	4700 / 54
CS HEV Cycle Life, 50 Wh Profile	Cycles	300,000		300,000	
Calendar Life, 35°C	year	15	10	15	10
Maximum System Weight	kg	60	90	120	160
Maximum System Volume	Liter	40	TBD	80	100
Maximum Operating Voltage	Vdc	400	420	400	410
Minimum Operating Voltage	Vdc	>0.55 x Vmax	170	>0.55 x Vmax	232
Maximum Self-discharge	Wh/day	50		50	5% in 60 Days
System Recharge Rate at 30°C	kW	1.4 (120V/15A)	1.4	1.4 (120V/15A)	3.6 (230V/16 A)
Unassisted Operating & Charging Temperature Range	°C	-30 to +52	-30 to +52	-30 to +52	-30 to +52
Survival Temperature Range	°C	-46 to +66	-46 to +66	-46 to +66	-46 to +66
Maximum System Production Price @ 100k units/yr	\$	\$1,700		\$3,400	

EFLEX EREV requires 2.5 times the power of USABC requirements



Electrode microstructure

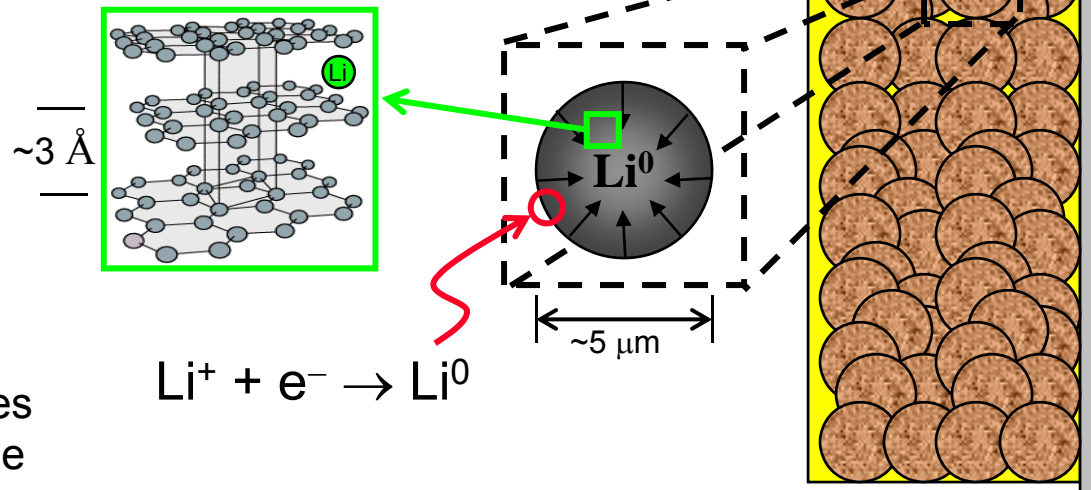


- Porous electrodes (~100 μm thick) composed of host particles (~1 to 5 μm diameter) are used to
 1. increase the surface area for reaction
 2. reduce lithium diffusion resistance

Anode charge reaction

1. Lithium ion is reduced at the electrode surface:

$$\text{Li}^+ + \text{e}^- \rightarrow \text{Li}^0$$
2. Lithium diffuses *rapidly* into host electrode through vacancies
 - Opposite reactions takes place at cathode particle surfaces





Lithium Intercalation of Carbon-Fiber Microelectrodes

Mark W. Verbrugge* and Brian J. Koch*

General Motors Research and Development Center, Physical Chemistry Department,
Warren, Michigan 48090-9055, USA

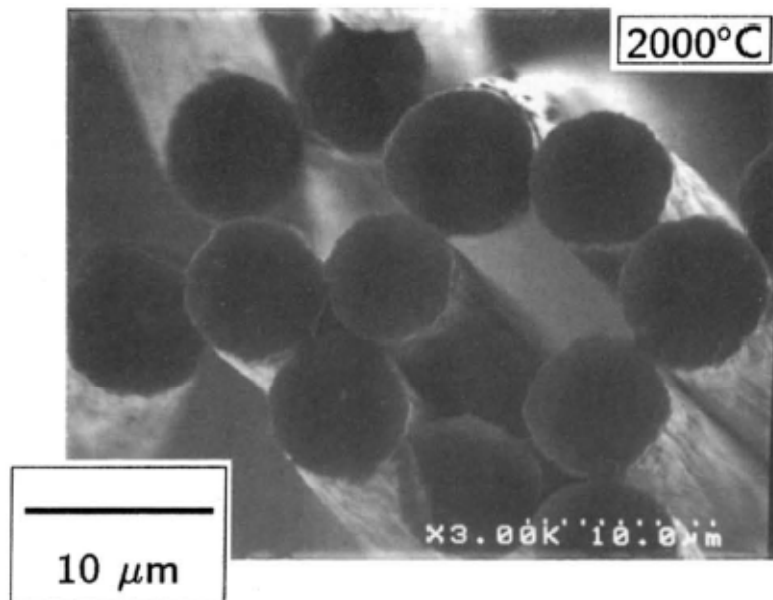


Fig. 2. Micrograph of fibers heat-treated for 4 h at 2000°C.

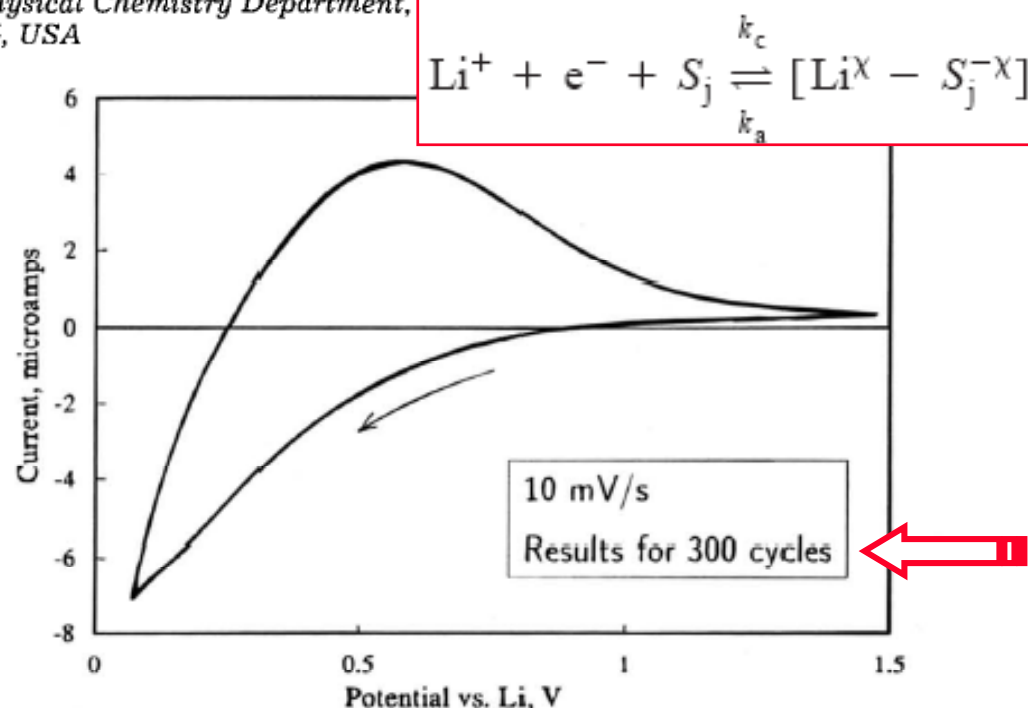


Fig. 3. Characteristic cyclic voltammogram. Data for 300 cycles are plotted.

- ❑ Ability of lamellar compounds of carbon to insert various species was well known by the later half of the 1800s (Schauffaütl, 1841...Sony, 1992)
- ❑ Aprotic solvents with high dielectric constants: W.S. Harris, Ph.D. Thesis, University of CA, Berkeley, 1958.
- ❑ Single fiber electrode: phenomena associated with the fabrication of a porous electrode do not obfuscate the subsequent characterization...use the Scientific Method to isolate critical characteristics
- ❑ Extremely stable lithiated carbon anode and Li reference (there is *still* confusion around the stability of carbon lithiation!)

Lithium ion challenges: durability focus

❑ **Cost**

- Can we size pack closer to end-of-life requirements?
- Can we reduce materials & processes costs?

❑ **Life**

- How do electrodes fail?
- Can we develop an accelerated life test?

❑ **Temperature tolerance**

- Can we improve low temperature power?
- Why is battery life shorter at higher temperatures?

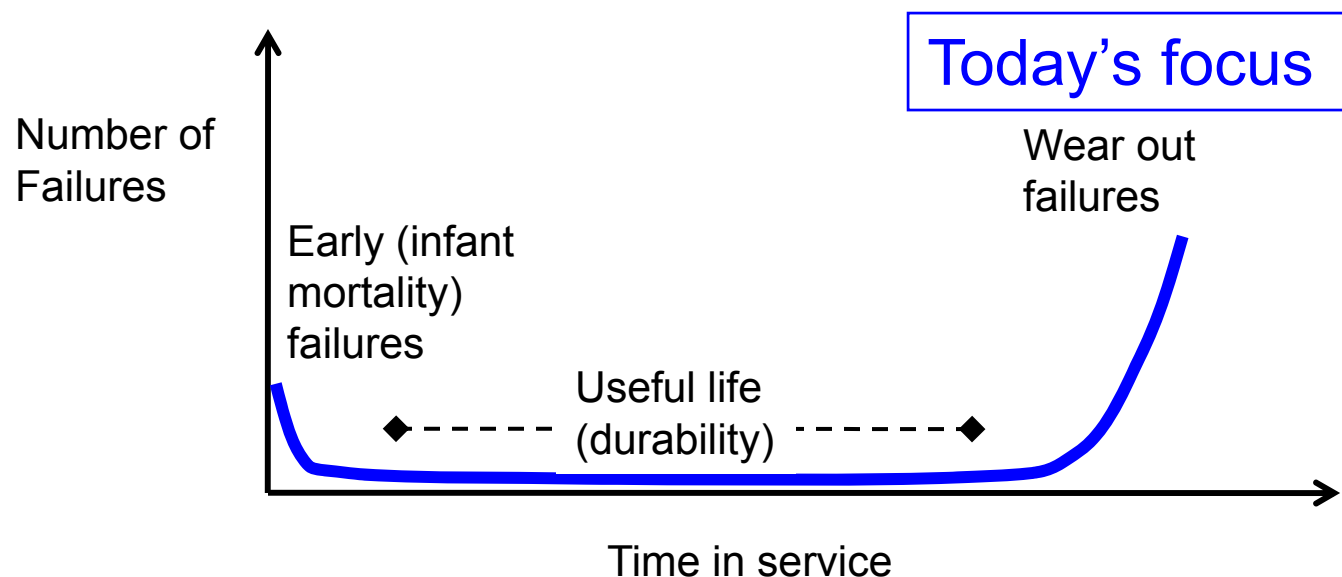
Durability...terminologies, *bathtub* curves

❑ Chemical degradation

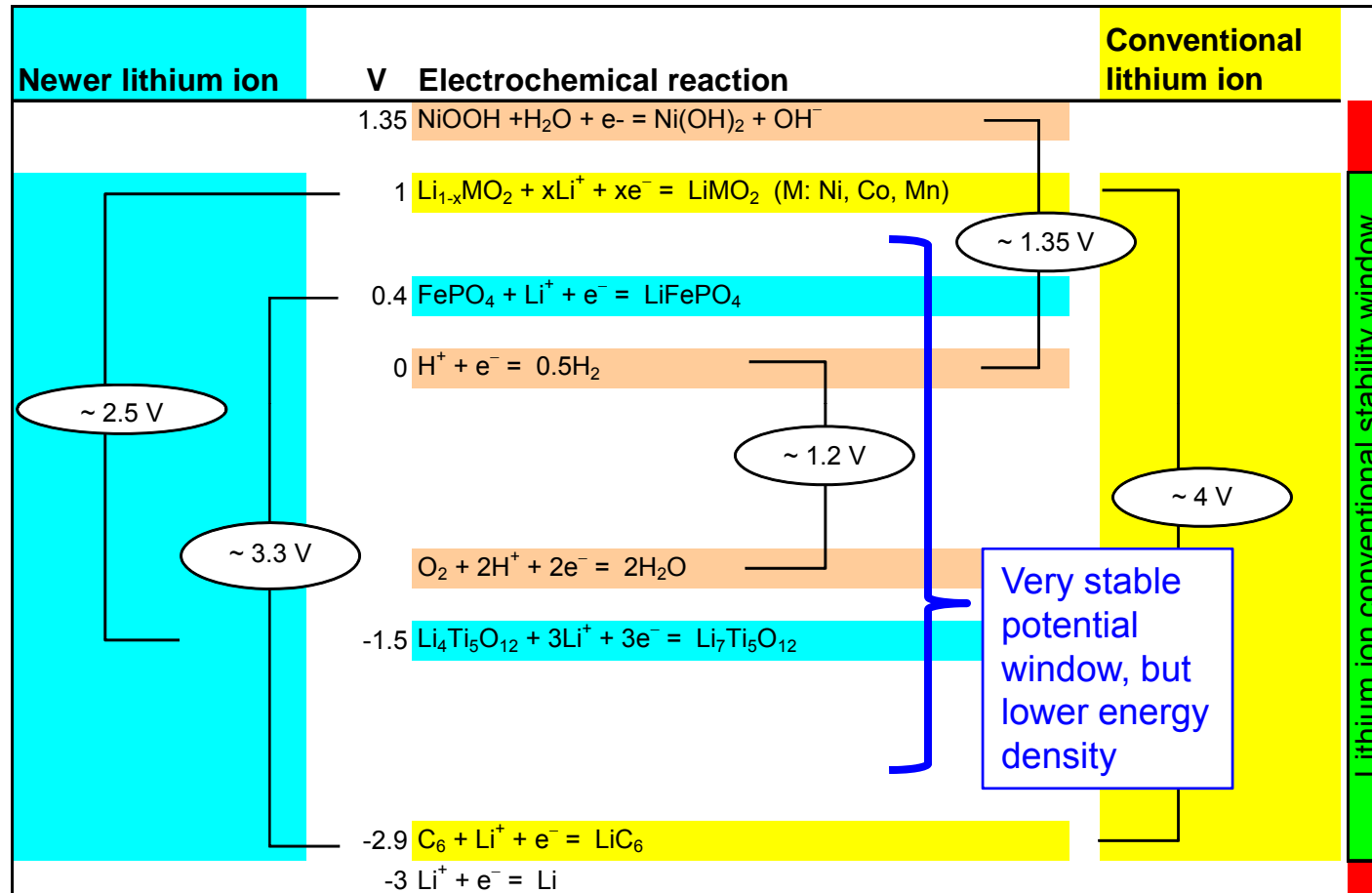
- Critical role of SEI (solid electrolyte interface) to impede deleterious degradation reactions within lithium ion cells
- **Calendar life** determined by chemical degradation

❑ Mechanical degradation

- Cyclic expansion and contraction of insertion or alloy materials leads to fatigue, cracking, and structural changes
- **Cyclic life** issues are affected by mechanical degradation and chemical degradation



Electrode potentials



- By changing an electrode voltage, new electrolytes can be employed with improved stability.
- For traction applications, conventional lithium ion cells still dominate...lower utilization for improved durability & abuse tolerance.

Negative electrode



ELSEVIER

Journal of Power Sources 110

www.elsevier.com/locate/jpowsour

Mathematical modeling of high-power-density insertion electrodes for lithium ion batteries

Mark W. Verbrugge^{a,*}, Daniel R. Baker^b, Brian J. Koch^c

^aGeneral Motors Research and Development Center, Warren, MI 48090-9055, USA

^bGeneral Motors Fuel Cell Propulsion Center, Warren, MI 48090-9055, USA

^cGeneral Motors Advanced Technology Vehicles, 1996 Technology Drive, Troy, MI 48067-7083, USA

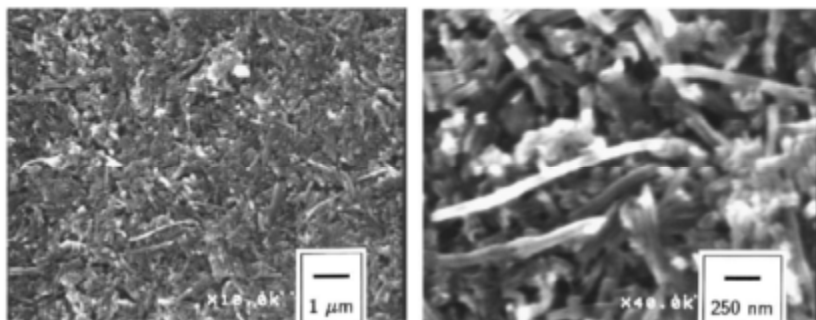
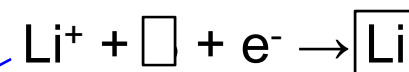
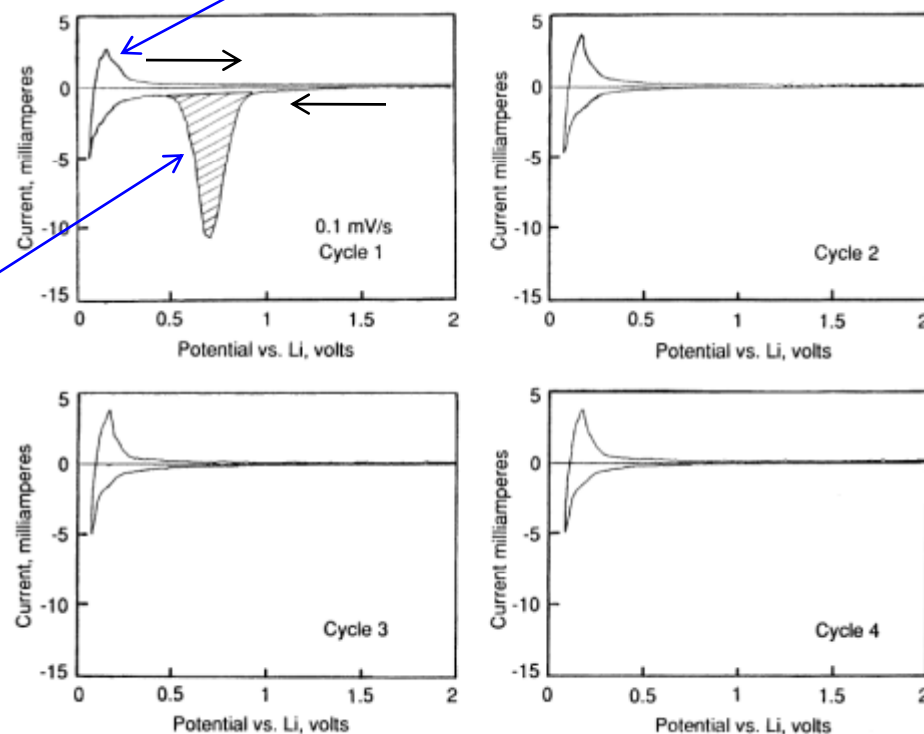
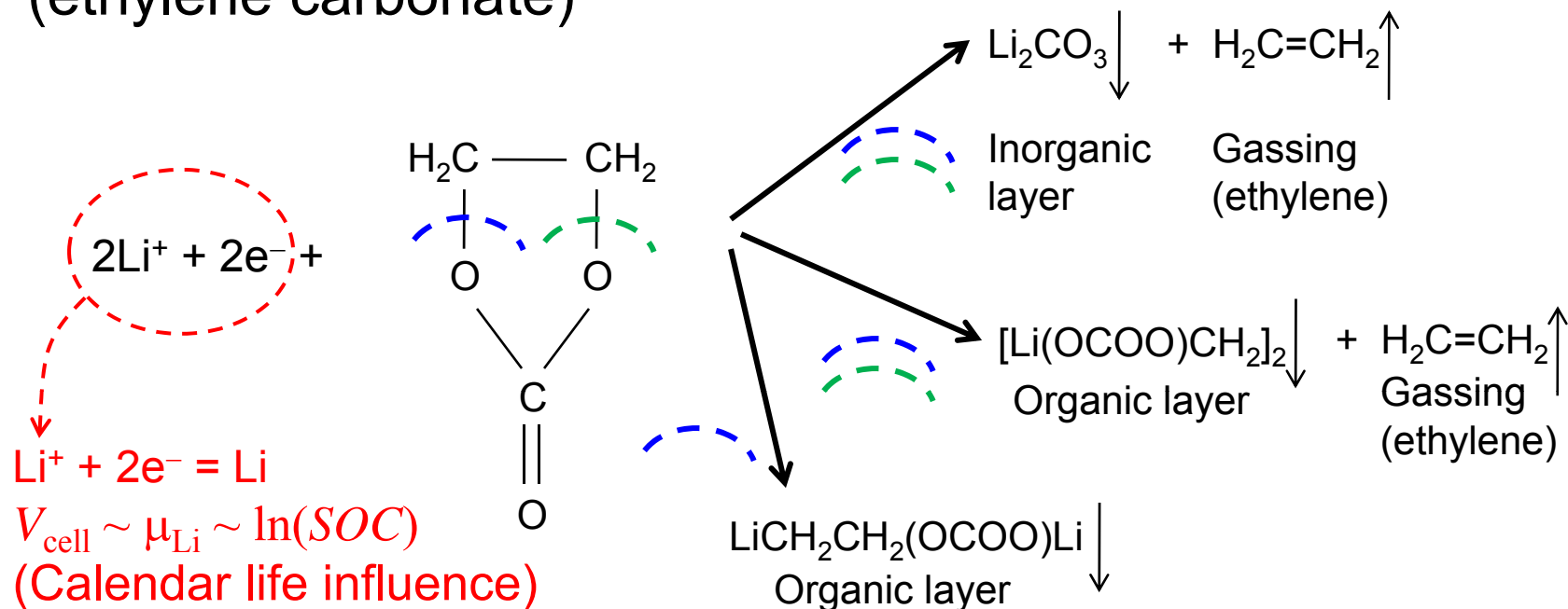


Fig. 3. High-magnification electrode micrographs.



- Solvent reduction at ~0.8V vs Li on first cycle
- Then ~100% Coulombic efficiency
- Next slide for more detail

Formation of the SEI...solvent reduction (ethylene carbonate)



□ Example reactions only...many others contribute to the formation of the solid electrolyte layer

- For computed IR spectra of surface species in an EC electrolyte, see S. Matsuta, T. Asada, and K. Kitaura. *J. Electrochem. Soc.* 147(2000)1695-1702...dimers found to be lowest energy
- Experimental FTIR data indicates predominance of $[\text{Li}(\text{OCOO})\text{CH}_2]_2$ for EC and EC+DEC systems with 1M LiPF_6 , see C. R. Yang, Y. Y. Wang, C. C. Wan, *J. Power Sources*, 72(1998)66.



ELSEVIER

Journal of Power Sources 97–98 (2001) 104–106

JOURNAL OF
**POWER
SOURCES**

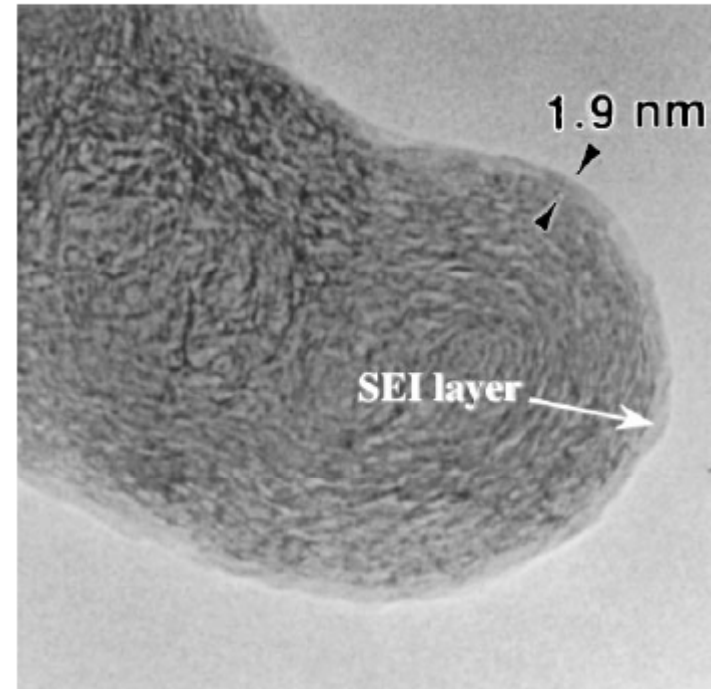
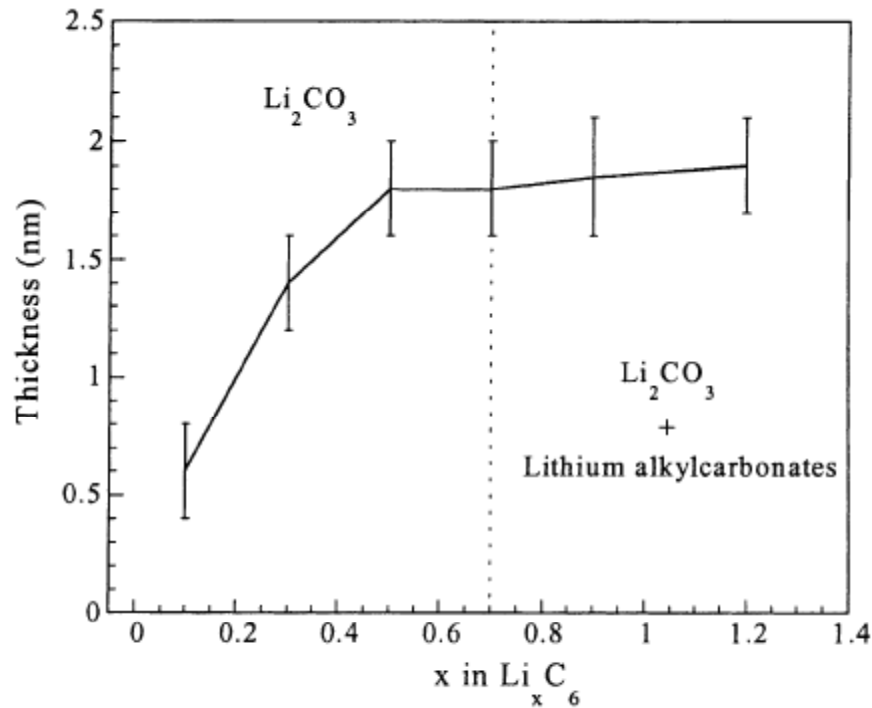
GM

www.elsevier.com/locate/jpowsour

In situ TEM study of the interface carbon/electrolyte

M. Dollé*, S. Grugeon, B. Beaudoin, L. Dupont, J-M. Tarascon

Laboratoire de Réactivité et de Chimie des Solides, UPRES A 6007, UPJV, 33 rue Saint-Leu, 80039 Amiens Cedex, France



The electrolyte used was LiPF_6 (1 M) in EC:DMC (1:1, w/w).

Electrochemical SPM investigation of the solid electrolyte interphase film formed on HOPG electrodes

D. Alliaata^{a,1}, R. Kötz^{a,*}, P. Novák^a, H. Siegenthaler^b

^aLaboratory for Electrochemistry, Paul Scherrer Institute, CH-5232 Villigen PSI, Switzerland

^bDepartment for Chemistry and Biochemistry, University of Bern, CH-3112 Bern, Switzerland

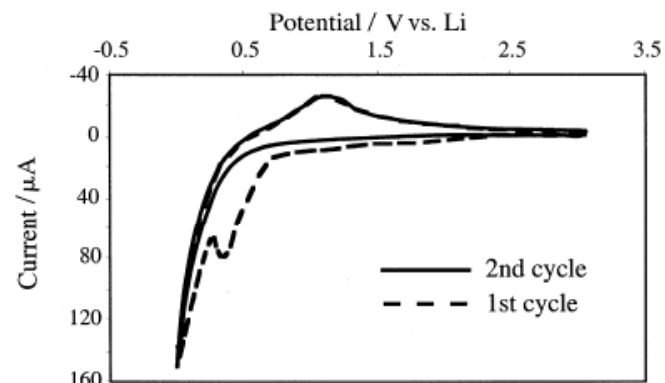
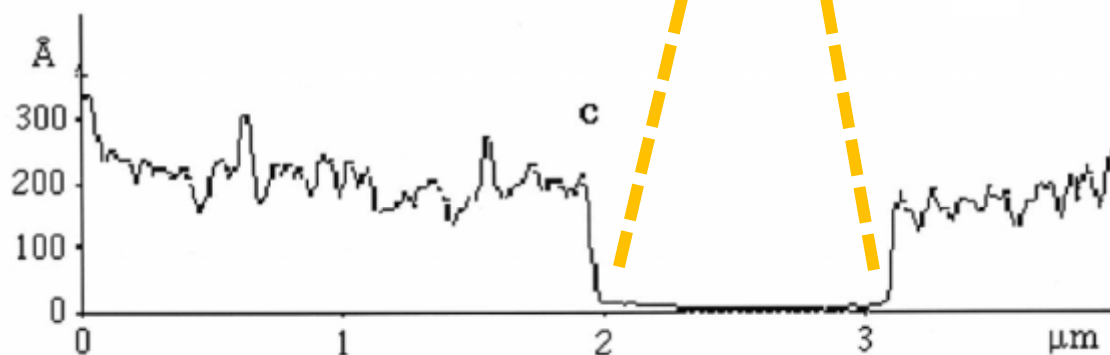
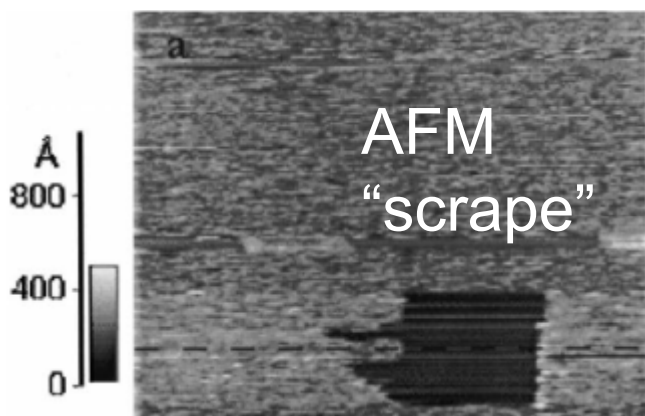


Fig. 1. CV curves recorded at 5 mV s^{-1} on HOPG in 1 M LiClO_4 in EC:DMC (dashed line, 1st cycle; solid line, 2nd cycle).

SEI grows to at least
20 nm in thickness
upon cycling



Contents lists available at ScienceDirect

Electrochimica Acta

journal homepage: www.elsevier.com/locate/electacta



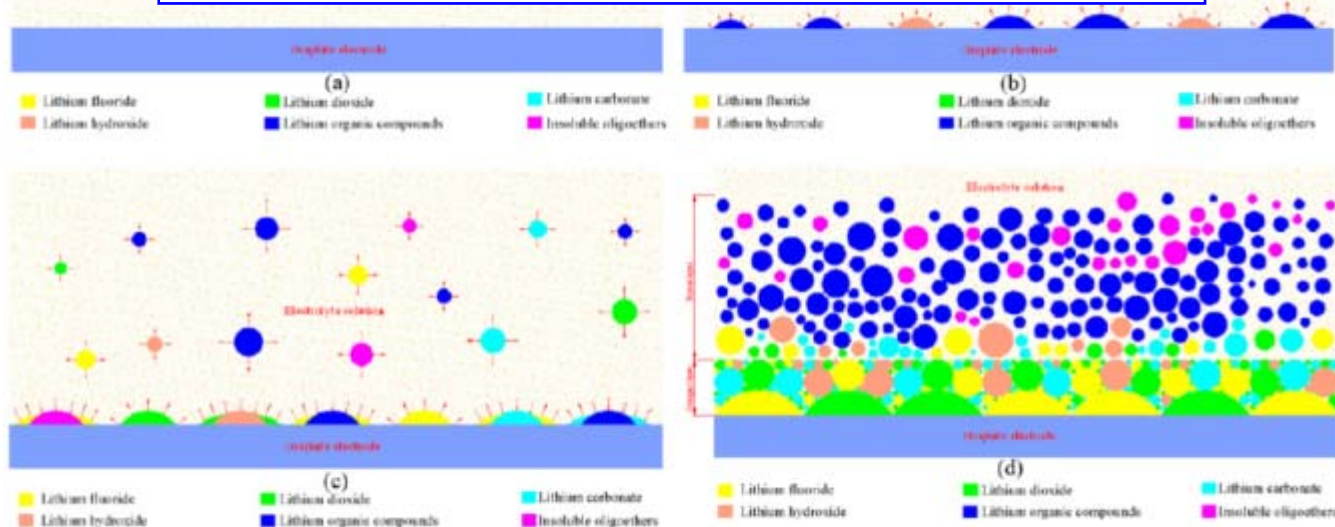
Phenomenologically modeling the formation and evolution of the solid electrolyte interface on the graphite electrode for lithium-ion batteries

Jian Yan^{a,b,*}, Bao-Jia Xia^a, Yu-Chang Su^b, Xiao-Zhong Zhou^b, Jian Zhang^a, Xi-Gui Zhang^a

^a Laboratory for Nano Sciences and Technologies, Shanghai Institute of Microsystem and Information Technology, Chinese Academy of Sciences, Shanghai 200050, PR China

^b School of Materials Science and Technology, Central South University, Changsha 410083, PR China

As a result, the constituents of the surface films nearest to the graphite surface will eventually be transformed to consist almost entirely of Li_2O and LiF in a mature SEI film.



Organic rich
Inorganic rich



A Mathematical Model for the Lithium-Ion Negative Electrode Solid Electrolyte Interphase

John Christensen^{*,z} and John Newman^{**}

Department of Chemical Engineering, University of California, Berkeley, California 94720, USA

$$L(t) - L_0 = At^m$$

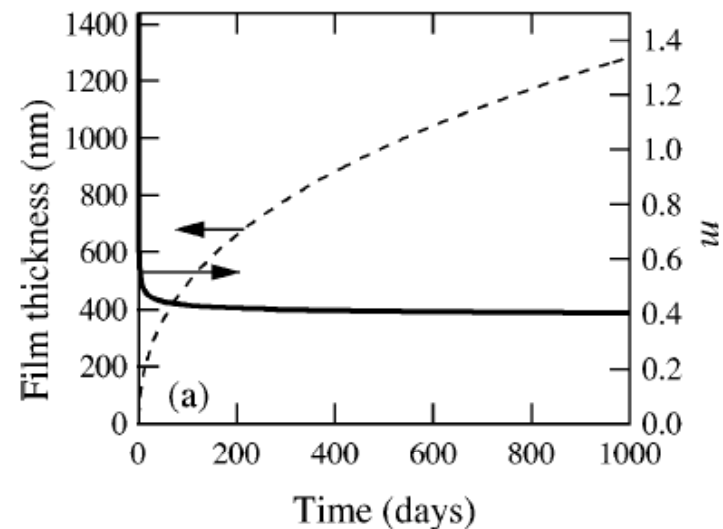
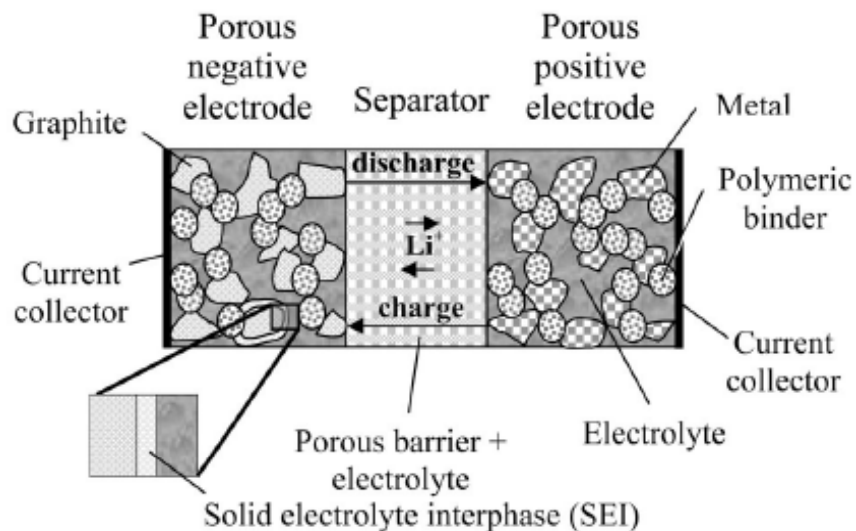
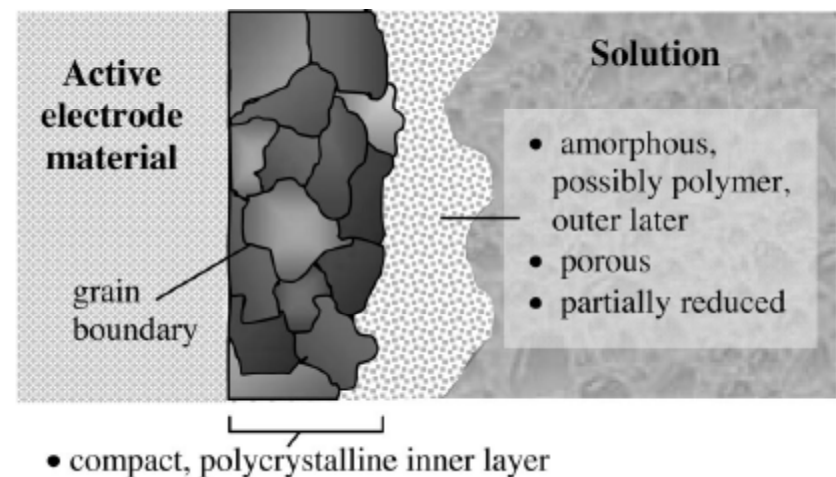


Figure 1. The lithium-ion battery, with two porous electrodes. The SEI layer on graphite is shown in the inset.

Resistance of the **inner inorganic layer** is modeled

Resistance of the **outer organic layer** is ignored



Positive electrode

Electrochemical oxidation of propylene carbonate (containing various salts) on aluminium electrodes

Kiyoshi Kanamura, Takashi Okagawa, Zen-ichiro Takehara

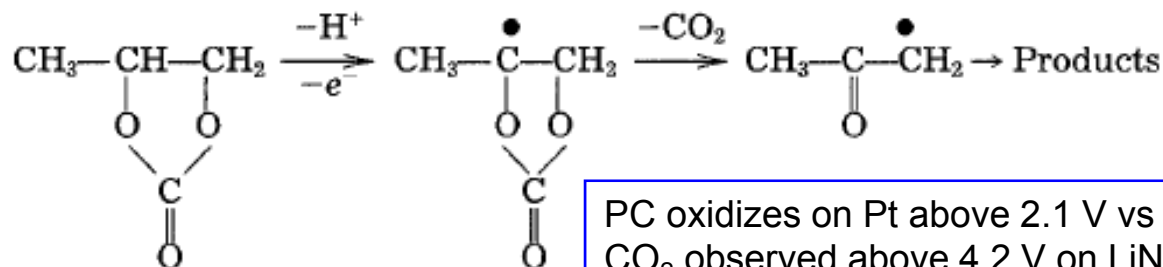
Division of Energy and Hydrocarbon Chemistry, Graduate School of Engineering, Kyoto University, Yoshida-honmachi, Sakyo-ku, Kyoto 606-01, Japan

Received 28 July 1995; accepted 11 September 1995

Petr Novák¹ and Wolf Vielstich*

Institute of Physical Chemistry, University of Bonn, D-5300 Bonn 1, Germany

J. Electrochem. Soc., Vol. 137, No. 6, June 1990



PC oxidizes on Pt above 2.1 V vs Li (forms lithium adducts).
 CO₂ observed above 4.2 V on LiNiO₂, above 4.8 V on LiCoO₂, LiMn₂O₄
 - Imhof & Novák, *J. Electrochem. Soc.*, 146(1999)1702.

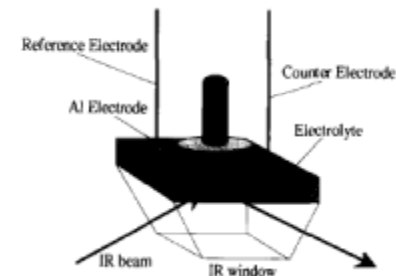


Fig. 1. Schematic of in situ FT-IR measurement for electrochemical oxidation of non-aqueous electrolytes on an aluminium electrode.

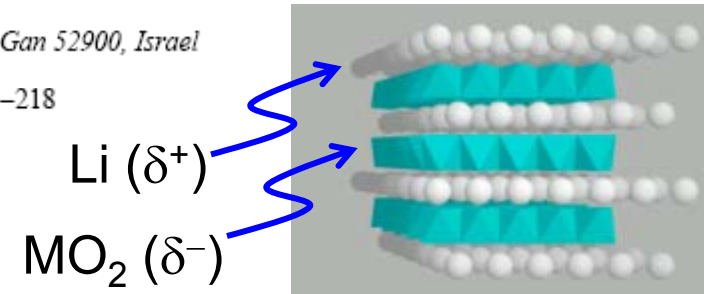
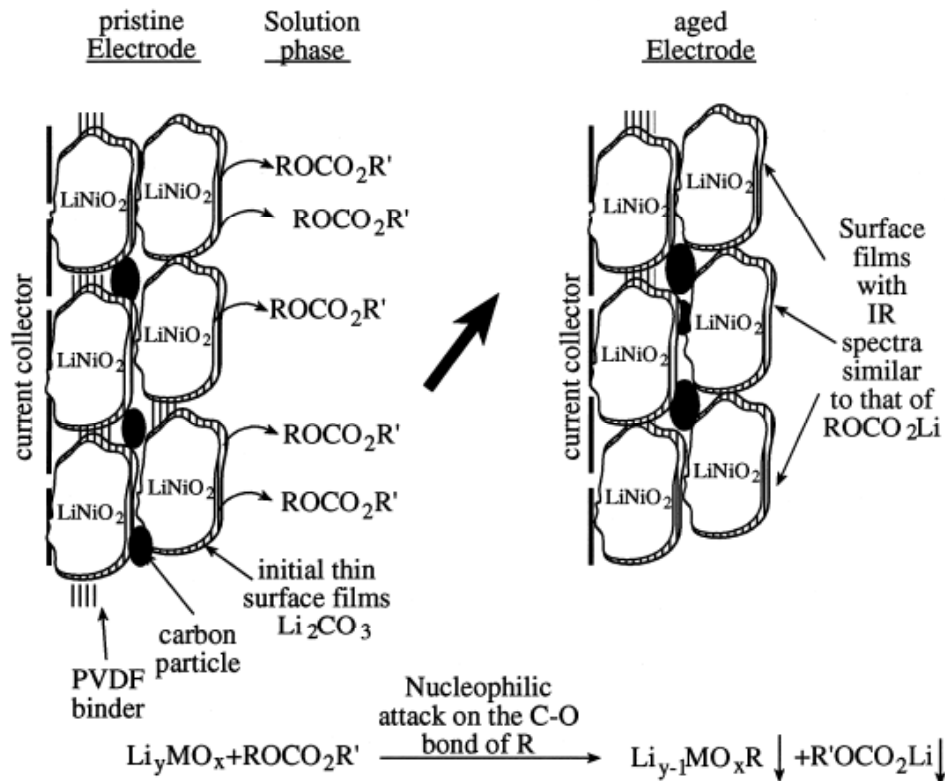
Review of selected electrode–solution interactions which determine the performance of Li and Li ion batteries

Doron Aurbach*

Department of Chemistry, Bar-Ilan University, Ramat-Gan 52900, Israel

Journal of Power Sources 89 (2000) 206–218

Surface film formation on cathode materials Option I : Nucleophilic reactions



❑ Growth of passive film on the positive electrode surface

❑ Li adducts (SEI) at low potentials (low SOC)

- Similar to SEI formation on carbon
- CO₂ evolution at high potentials (over-charge)

❑ High SOC, less Li, and oxygens can release

Review of selected electrode–solution interactions which determine the performance of Li and Li ion batteries

Doron Aurbach *

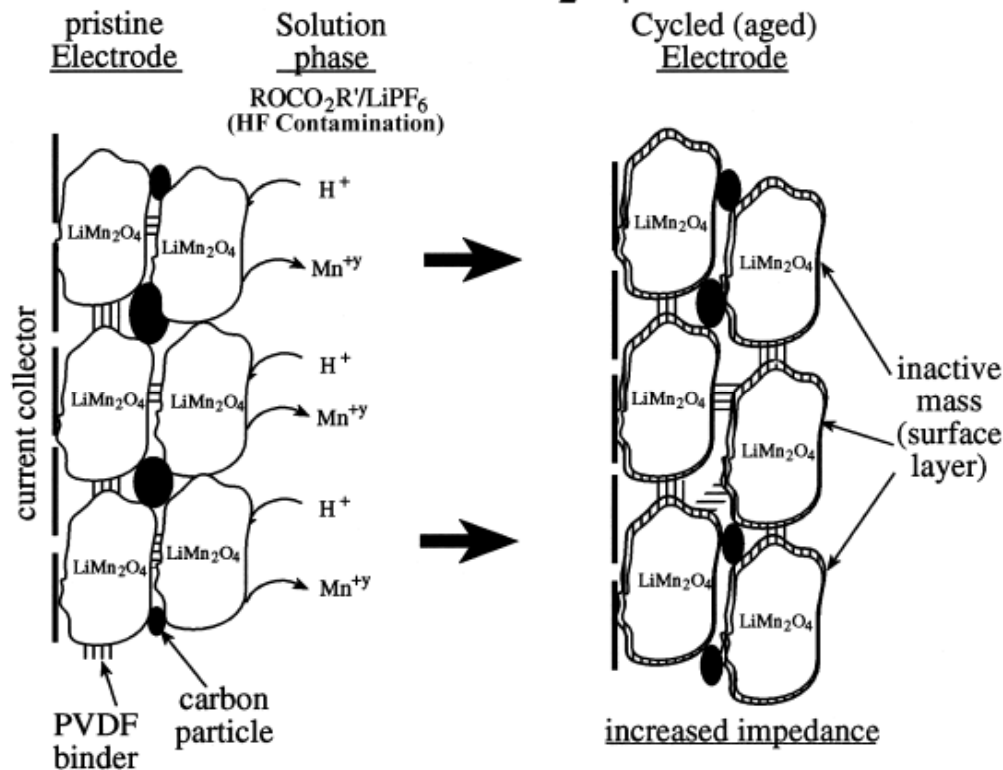
Department of Chemistry, Bar-Ilan University, Ramat-Gan 52900, Israel

Journal of Power Sources 89 (2000) 206–218

Surface film formation on cathode materials

Option II : Exchange reactions, formation of inactive mass

Example 1 LiMn_2O_4 spinel

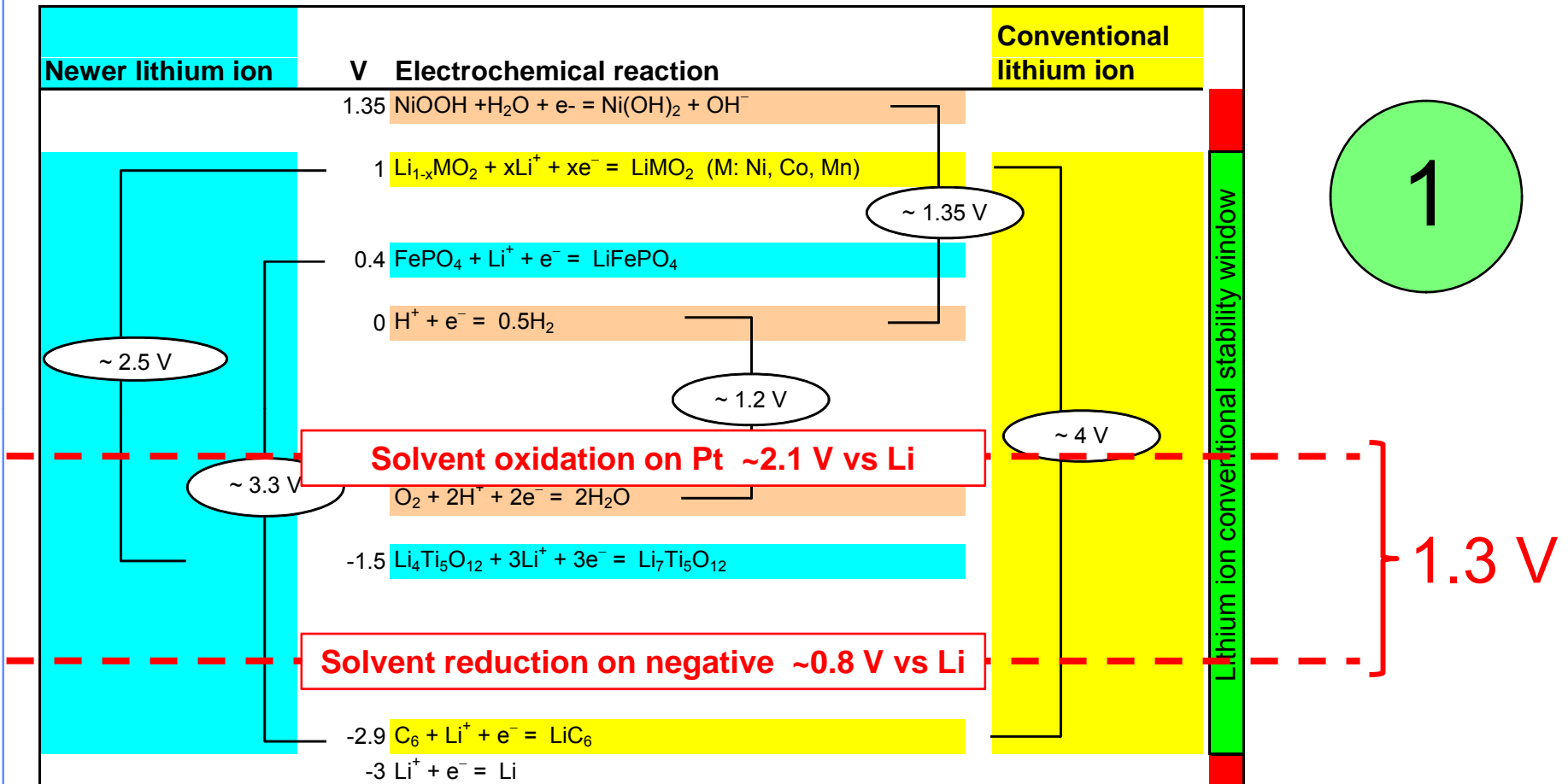


❑ Growth of passive film on the LMO surface

❑ Dissolved Mn²⁺ transports to the negative electrode and breaks down the SEI

- This problem can also occur with Fe dissolution within iron phosphate cells

Summary: role of surface layers on + and -



❑ Underscores the importance of the SEI

- Disruption of the SEI (e.g., due to dilation, crack propagation, etc.) is deleterious to cell life...even low reaction rates are a problem
 - Loss of Li
 - Gas generation

Life modeling (cell)



ELSEVIER

An accelerated calendar and cycle life study of Li-ion cells

I. Bloom^{a,*}, B.W. Cole^a, J.J. Sohn^a, S.A. Jones^a, E.G. Polzin^a, V.S. Battaglia^a, G.L. Henriksen^a,
C. Motloch^b, R. Richardson^b, T. Unkelhaeuser^c, D. Ingersoll^c, H.L. Case^c

^aElectrochemical Technology Program, Argonne National Laboratory, 9700 South Cass Avenue, Argonne, IL 60439, USA

^bIdaho National Engineering and Environmental Laboratory, Idaho Falls, ID 83415, USA

^cSandia National Laboratories, Albuquerque, NM 87185, USA

Cell chemistry

Positive electrode

8 wt.% PVDF binder
4 wt.% SFG-6 graphite
4 wt.% carbon black
84 wt.% LiNi_{0.8}Co_{0.2}O₂

Negative electrode

9 wt.% PVDF binder
16 wt.% SFG-6 graphite
75 wt.% MCMB-6 graphite

Electrolyte

1 M LiPF₆ in EC/DEC (1:1)

Separator

37 μm thick PE Celgard separator

Table 9

Calculated times to 20% power loss

Test/group	Time to 20% power fade (weeks)
40% SOC calendar life	387.21
60% SOC/A calendar life	127.64
60% SOC/B calendar life	39.37
80% SOC calendar life	11.33
60% SOC, 3% ΔSOC cycle life	6.91
60% SOC, 6% ΔSOC cycle life	0.99
80% SOC, 3% ΔSOC cycle life	38.72
80% SOC, 6% ΔSOC cycle life	1.94

The data were fit by the general equation

$$Q = A \exp\left(\frac{-E_a}{RT}\right) t^z$$

where Q is the ASI or power, A the pre-exponential factor, E_a the activation energy in J , R the gas constant, T the absolute temperature, t the time, and z the exponent of time. For simple diffusion control or layer growth, $z = 1/2$. This



ELSEVIER

Aging mechanism in Li ion cells and calendar life predictions

M. Broussely^{a,*}, S. Herreyre^b, P. Biensan^b, P. Kasztejna^c,
K. Nechev^c, R.J. Staniewicz^c

^aSAFT BP 1039, 86060 Poitiers, France

^bSAFT, 111 Blvd A. Daney, 33074 Bordeaux, France

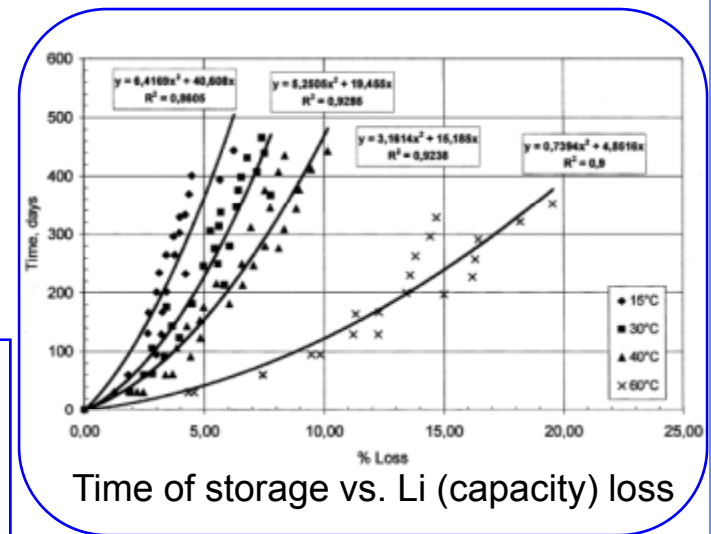
^cSAFT America, 107 Beaver court, Cockeysville, MD, USA

The most commonly adopted picture is that the interface layer is considered as a solid electrolyte interphase (SEI) being a good ionic but poor electronic conductor, as proposed by Peled [4].

$$\frac{dx}{dt} = kX = \frac{k\chi s}{e} \quad (1)$$

where x is the number of moles of Li being reacting, χ the specific conductivity, s the interface area and e is the layer thickness.

$$t = e^{[(4661/T)-14]} x^2 + e^{[(4437/T)-11.6]} x$$



The “5 Ah” prismatic cell used a stainless steel can and was configured as can negative. The chemistry was LiCoO₂/EC-DEC-DMC 1 M LiPF₆ + VC additive/synthetic graphite.

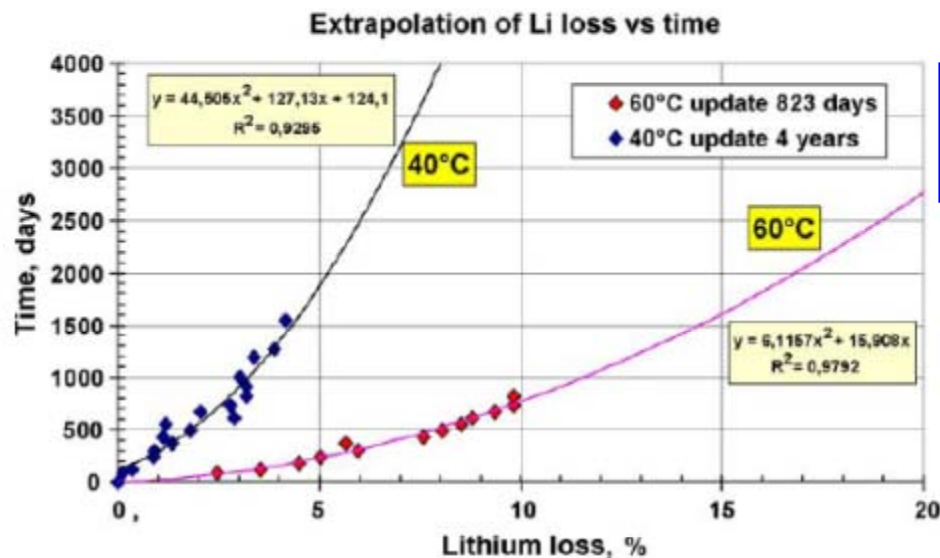
Main aging mechanisms in Li ion batteries

M. Broussely^{a,*}, Ph. Biensan^b, F. Bonhomme^b, Ph. Blanchard^b,
S. Herreyre^b, K. Nechev^c, R.J. Staniewicz^c

^a Saft, BP 1039, 86060 Poitiers, France

^b Saft 111 Bvd. A. Daney, 33000 Bordeaux, France

^c Saft America, 107 Beaver Court, Cockeysville, MD, USA



Both cells use the $\text{LiNi}_x\text{Co}_y\text{Al}_z\text{O}_2/\text{graphite} + \text{PC/EC/DMC} + 1 \text{ M LiPF}_6$ chemistry.

Fig. 8. Storage time on float (3.9 V) at 60 and 40 °C vs. lithium loss. Saft “Industrial” Li ion Ni-based cells.



ELSEVIER

Journal of Power Sources 113 (2003) 72–80

JOURNAL OF
**POWER
SOURCES**

GM

www.elsevier.com/locate/jpowsour

Simulation of capacity fade in lithium-ion batteries

R. Spotnitz*

Battery Design Co., 2277 DeLucchi Dr., Pleasanton, CA 94588, USA

- (1) Capacity loss on storage has reversible and irreversible components.
- (2) Capacity loss on storage or cycling increases with increasing temperature.
- (3) Capacity loss on storage increases with increasing cell voltage.
- (4) Cycling causes capacity loss at a greater rate than storage.
- (5) Capacity loss can correlate with cell impedance.

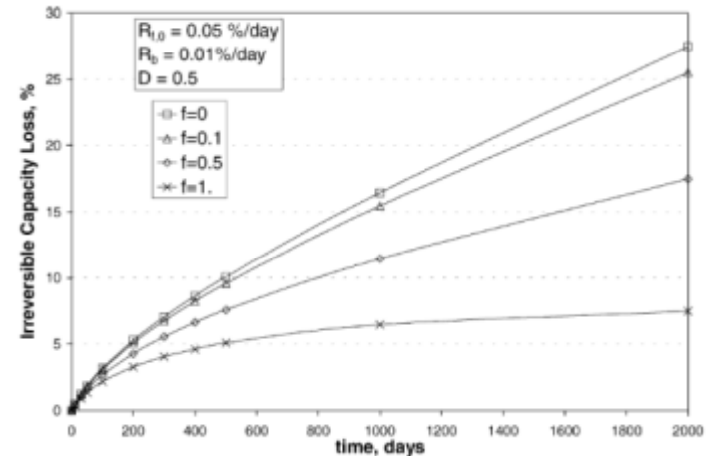


Fig. 5. Effect of Li^+ ion recovery from SEI on irreversible capacity loss.

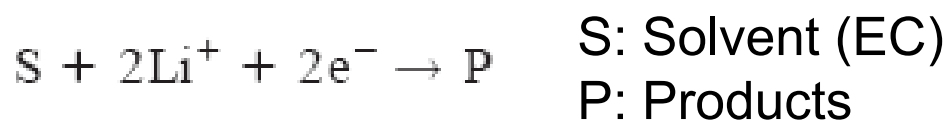
5.3. Irreversible and irreversible capacity loss due to SEI growth and dissolution

$$t = - \left(\frac{R_{f,0} - R_b}{R_b^2 D} \right) \left[1 - \exp \left(- \frac{R_b N_{\text{loss}} D}{R_{f,0}} \right) \right] + \frac{N_{\text{loss}}}{R_b}$$

Development of First Principles Capacity Fade Model for Li-Ion Cells

P. Ramadass,* Bala Haran,** Parthasarathy M. Gomadam,* Ralph White,***
and Branko N. Popov**,*z

Department of Chemical Engineering, University of South Carolina, Columbia, South Carolina 29208, USA



- Butler-Volmer equation for solvent reduction
- Film-growth model for SEI resistance...**Power**
- Lithium loss model for capacity loss...**Capacity**
- Note: This is treats chemical degradation
 - No influence due to expansion and contraction of the host material

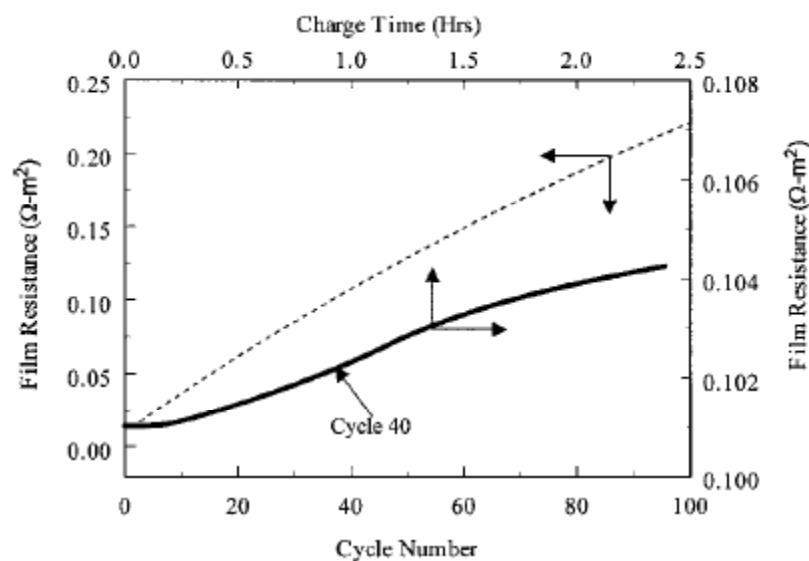


Figure 5. Variation of film resistance during charging for (solid line) cycle 40 and (dotted lines) variation of film resistance with cycle number.

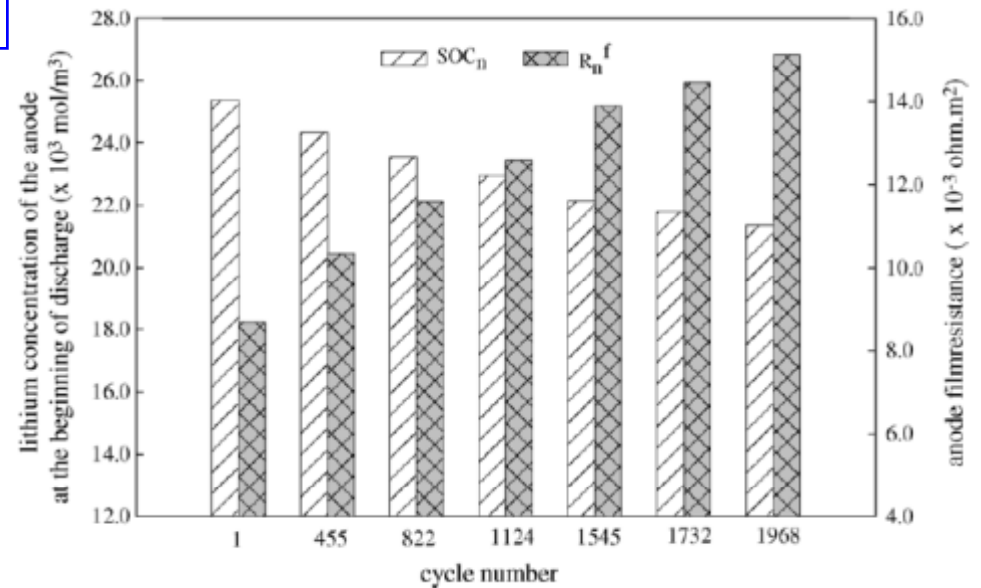
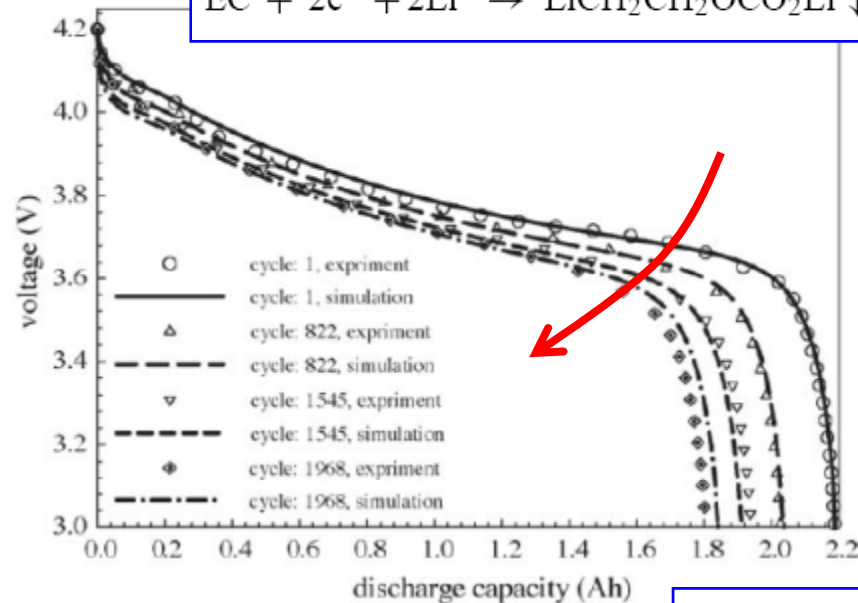
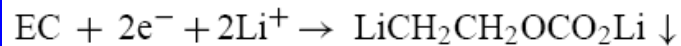
A generalized cycle life model of rechargeable Li-ion batteries

Gang Ning, Ralph E. White, Branko N. Popov*

Department of Chemical Engineering, University of South Carolina, Columbia, SC 29208, USA

Resistance of the **outer organic layer** is modeled

Resistance of the **inner inorganic layer** is ignored



$$j_{\text{para}} = -j_{\text{para}}^0 \exp\left(\frac{\alpha_c F}{RT} \eta\right)$$

$$\eta = \phi_s - \phi_e - U_{\text{para}} - jR_f$$

$$\frac{\partial \delta_f}{\partial t} = -\frac{j_{\text{para}} | \times M}{\rho \times F}$$

$$R_s | N = \frac{\delta_f | N}{\kappa}$$

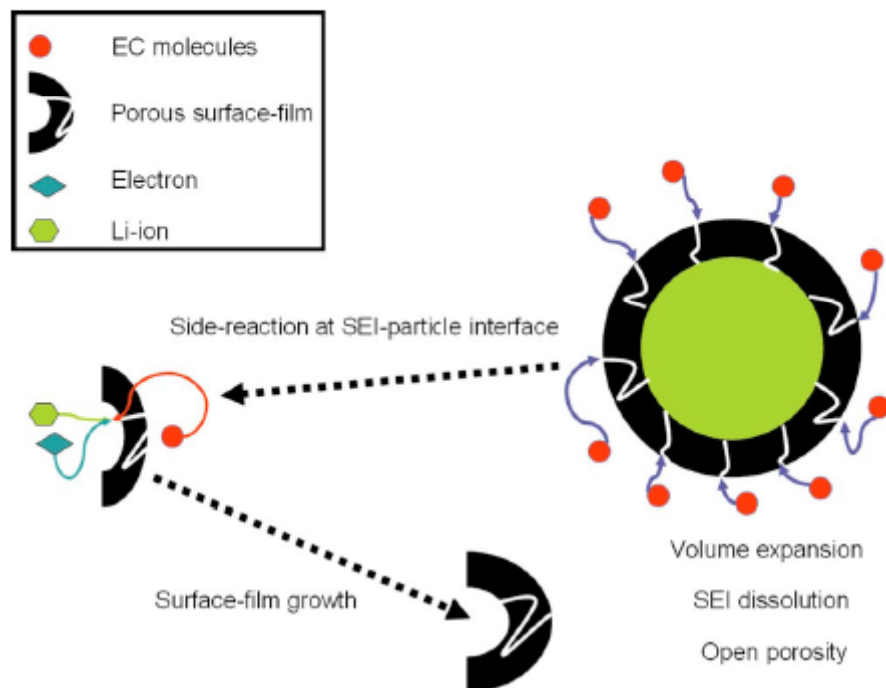
$$Q_s = \left| \int_{t=0}^{t=t_{\text{para}}} j_{\text{para}} a_{s,n} dt \right|$$

Multimodal Physics-Based Aging Model for Life Prediction of Li-Ion Batteries

M. Safari,^a M. Morcrette,^a A. Teyssoit,^b and C. Delacourt^{a,*}

^aLaboratoire de Réactivité et Chimie des Solides, Université de Picardie Jules Verne, 80039 Amiens Cedex, France

^bRenault Research Department, 78288 Guyancourt, France



Resistance of the
outer organic layer is
modeled

Resistance of the
inner inorganic layer
is ignored

Figure 1. (Color online) Physical picture for SEI growth at the anode particle surface.

Multimodal Physics-Based Aging Model for Life Prediction of Li-Ion Batteries

M. Safari,^a M. Morcrette,^a A. Teyssoit,^b and C. Delacourt^{a,b,*}

^aLaboratoire de Réactivité et Chimie des Solides, Université de Picardie Jules Verne, 80039 Amiens Cedex, France

^bRenault Research Department, 78288 Guyancourt, France

Governing equations

$$i_{\text{int}} = Fk_{\text{int}}^{\text{O,app}} c_{\text{Li}}^{\beta} (c_{\text{Li}}^{\text{max}} - c_{\text{Li}})^{1-\beta} \left\{ \exp \left[\frac{(1-\beta)F}{RT} \left(\Phi_1 - U - \frac{\delta}{\kappa_{\text{SEI}}} i_t \right) \right] - \exp \left[-\frac{\beta F}{RT} \left(\Phi_1 - U - \frac{\delta}{\kappa_{\text{SEI}}} i_t \right) \right] \right\}$$

$$\frac{\partial c_{\text{Li}}}{\partial t} = \frac{1}{r^2} \frac{\partial}{\partial r} \left(D_{\text{Li}} r^2 \frac{\partial c_{\text{Li}}}{\partial r} \right)$$

$$i_s = -Fk_{f,s} c_{\text{EC}} \exp \left[-\frac{\beta_s F}{RT} \left(\Phi_1 - \frac{\delta}{\kappa_{\text{SEI}}} i_t \right) \right]$$

$$i_t = i_{\text{int}} + i_s$$

$$\frac{\partial c_{\text{EC}}}{\partial t} = D_{\text{EC}} \frac{\partial^2 c_{\text{EC}}}{\partial r^2} - \frac{d\delta}{dt} \frac{\partial c_{\text{EC}}}{\partial r}$$

$$\frac{d\delta}{dt} = -\frac{i_s M_{\text{SEI}}}{2F \rho_{\text{SEI}}}$$

Boundary conditions

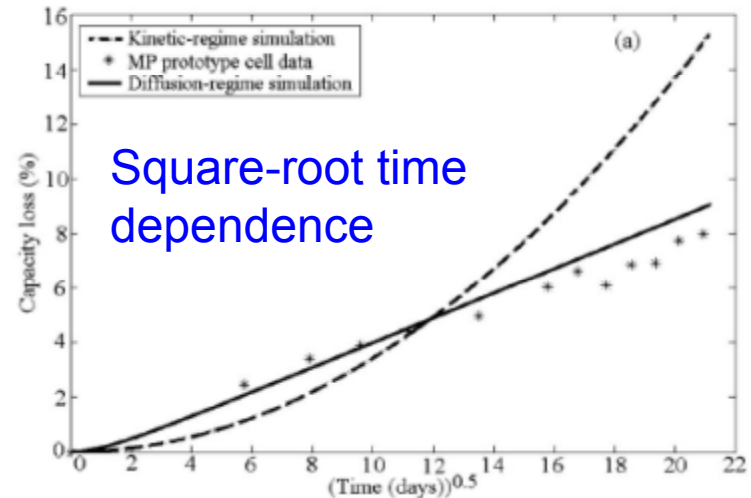
$$\left. \frac{\partial c_{\text{Li}}}{\partial r} \right|_{r=0} = 0$$

$$\left. \frac{\partial c_{\text{Li}}}{\partial r} \right|_{r=R} = -\frac{i_{\text{int}}}{FD_{\text{Li}}}$$

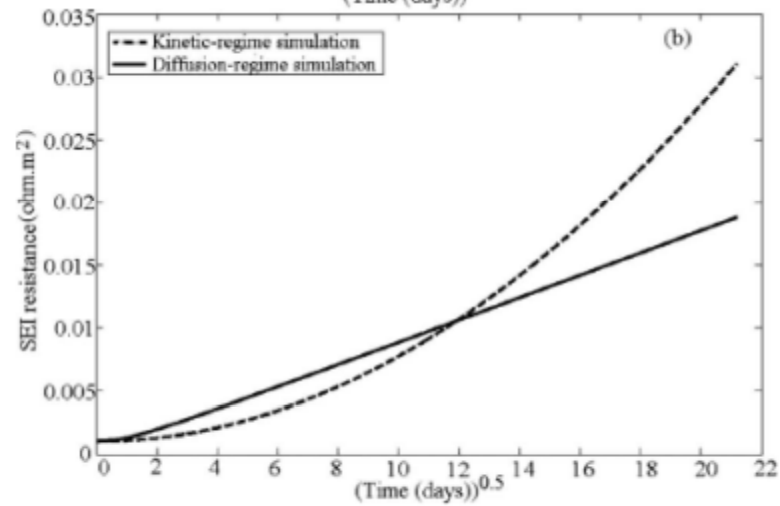
$$-D_{\text{EC}} \left. \frac{\partial c_{\text{EC}}}{\partial r} \right|_{r=R} + \nu c_{\text{EC}} \Big|_{r=R} = \frac{i_s}{F}$$

$$c_{\text{EC}} \Big|_{r=R+\delta} = \varepsilon_{\text{SEI}} c_{\text{EC,sln}}$$

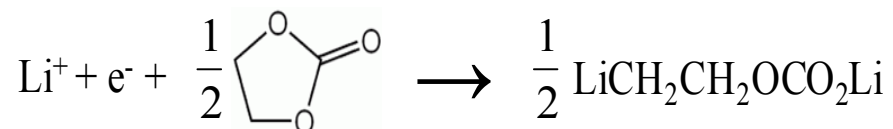
□ Electrochemical degradation model



Square-root time dependence

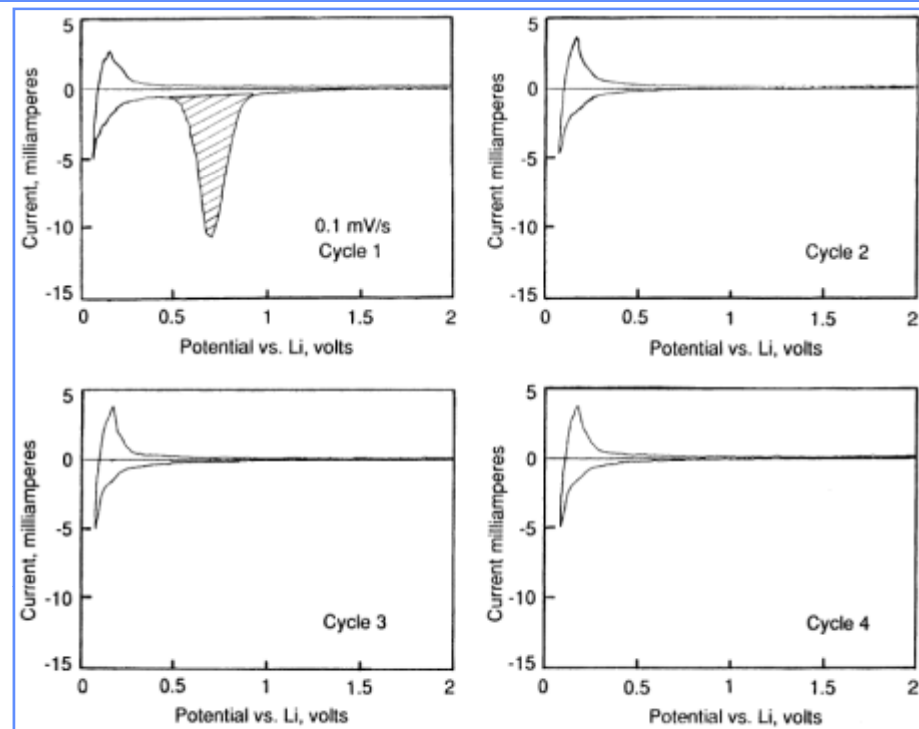


On the importance of coulombic efficiency η_I



Cycle	Capacity
1	$(Ah_0)\eta_I$
2	$[(Ah_0)\eta_I]\eta_I$
3	$[(Ah_0)\eta_I\eta_I]\eta_I$
⋮	
N	$(Ah_0)(\eta_I)^N$

2



For $N = 5000$ cycles and a 12/16 or 75% capacity retention, the current efficiency per cycle must be such that

$$[Ah_0(\eta_I)^N]/Ah_0 > 0.75, \text{ or } \eta_I > (0.75)^{(1/5000)}, \text{ hence } \eta_I > 0.99994.$$

- This is why very low rates of lithium-consuming reactions can lead to premature cell failure. The rates can be so low that they are not measureable in terms of seeing current maxima associated with solvent reduction, for example.

*Second emphasis: **mechanical degradation** leading to wear out*



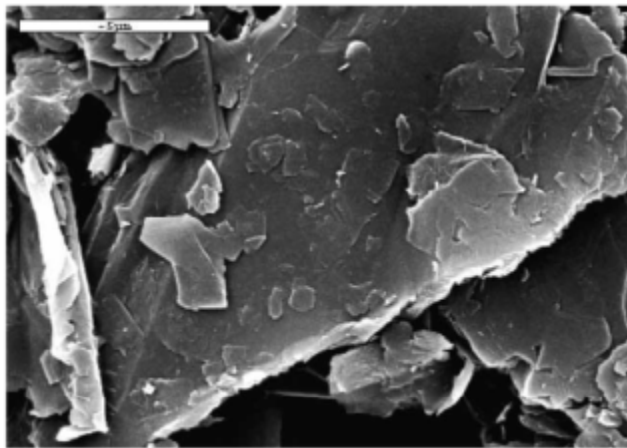
Capacity fading of lithiated graphite electrodes studied by a combination of electroanalytical methods, Raman spectroscopy and SEM

E. Markervich, G. Salitra, M.D. Levi, D. Aurbach *

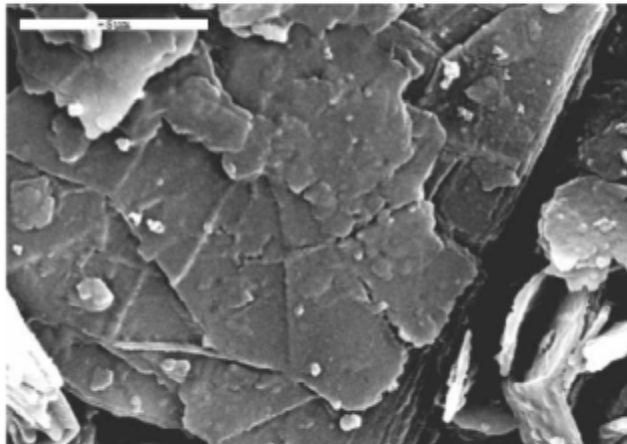
Department of Chemistry, Bar-Ilan University, 52900 Ramat-Gan, Israel

**NEGATIVE
ELECTRODE**

Journal of Power Sources 146 (2005) 146–150



(a)



(b)

SEM images of the surface of the KS-15 composite pristine electrode (a) and the same electrode after 140 intercalation–deintercalation cycles at 25 °C (b and c).

During cycling, **graphite particles crack into smaller pieces** that are less oriented than the original platelets, with the possible filling of the cracks thus formed by the reduction products of the electrolyte solution. In addition, the **average crystalline size (estimated by Raman spectroscopy) decreases** as cycling progresses.

Performance of LiNiCoO₂ materials for advanced lithium-ion batteries

POSITIVE ELECTRODE

Yuichi Itou, Yoshio Ukyo*

Toyota Central R&D Labs Inc., Nagakute, Aichi 480-1192, Japan

Available online 8 August 2005

Journal of Power Sources 146 (2005) 39–44

In this study, the deterioration mechanism of lithium-ion batteries using composite particles of LiNiCoO₂ as the positive electrode material is investigated. The

particles are formed in particles with large volume change resistance at positive electronic conduction, due to the large volume change. To verify this mechanism,



“This result indicates volume change causes the increase in resistance.”

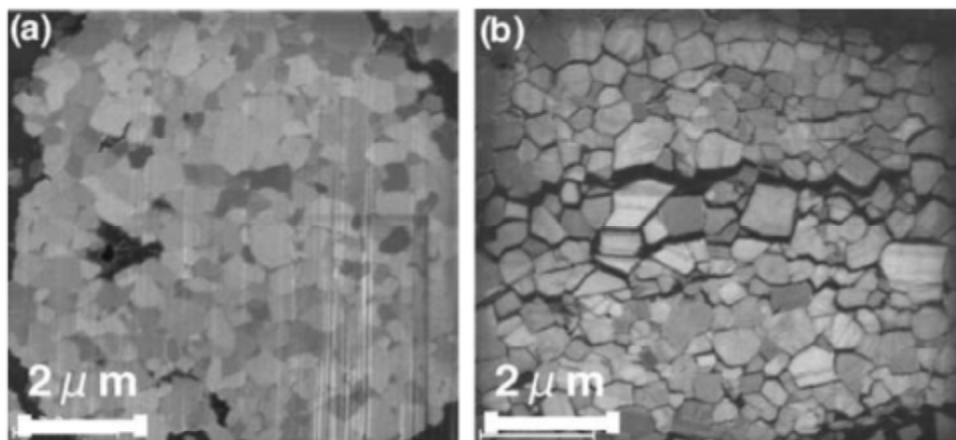
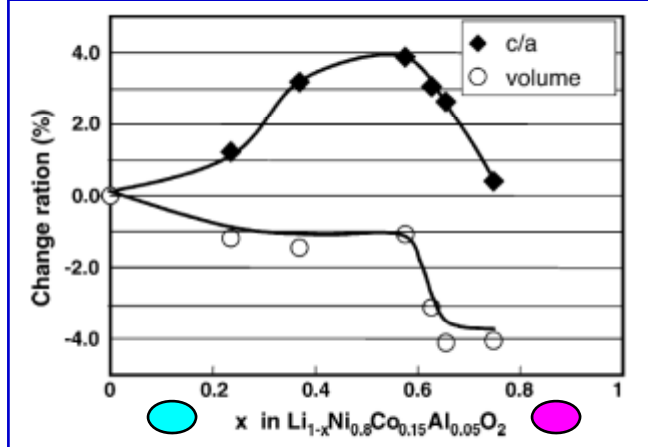


Fig. 9. Morphology of positive particle: (a) state of discharge, (b) state of charge.



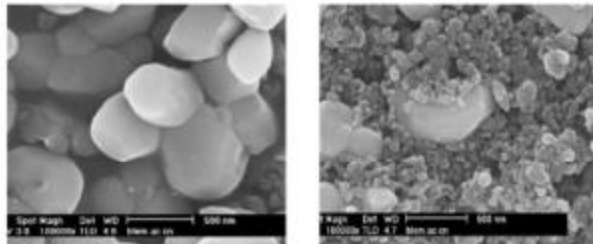


Cracking causing cyclic instability of LiFePO₄ cathode material

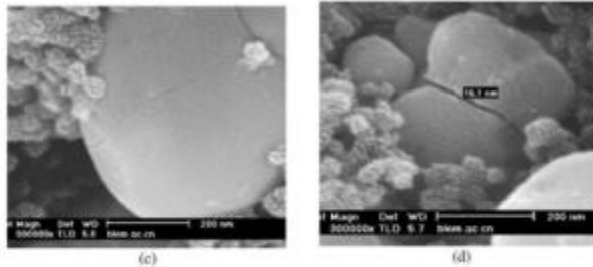
Deyu Wang, Xiaodong Wu, Zhaoxiang Wang, Liquan Chen*

Journal of Power Sources 140 (2005) 125–128

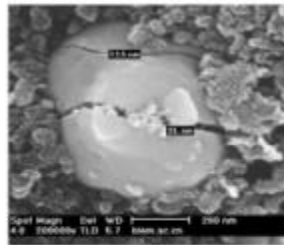
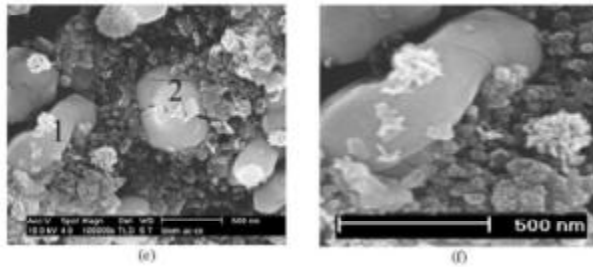
**POSITIVE
ELECTRODE**



Cycles	
0'	0
10	30
60	60_p1
	60_p2



LiFePO₄ possesses an olivine structure with three-dimensional network. The lattice constants of LiFePO₄ are $a = 10.33 \text{ \AA}$, $b = 6.01 \text{ \AA}$, $c = 4.69 \text{ \AA}$, $V = 291.2 \text{ \AA}^3$ and the lattice constants of FePO₄ are $a = 9.81 \text{ \AA}$, $b = 5.79 \text{ \AA}$, $c = 4.78 \text{ \AA}$, $V = 271.5 \text{ \AA}^3$, respectively [11]. The volume change of this phase transformation is 6.77%. The volume change is

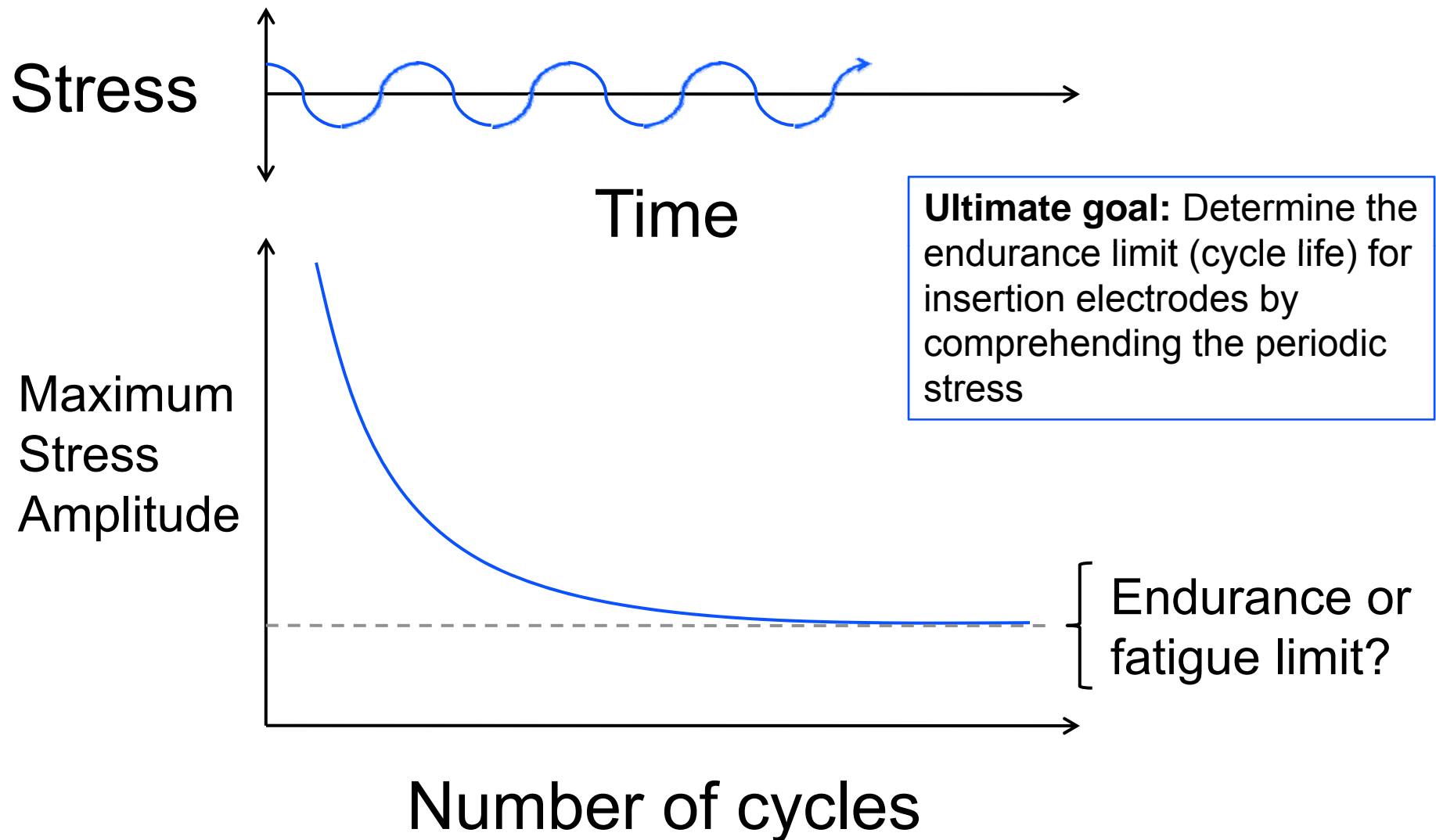


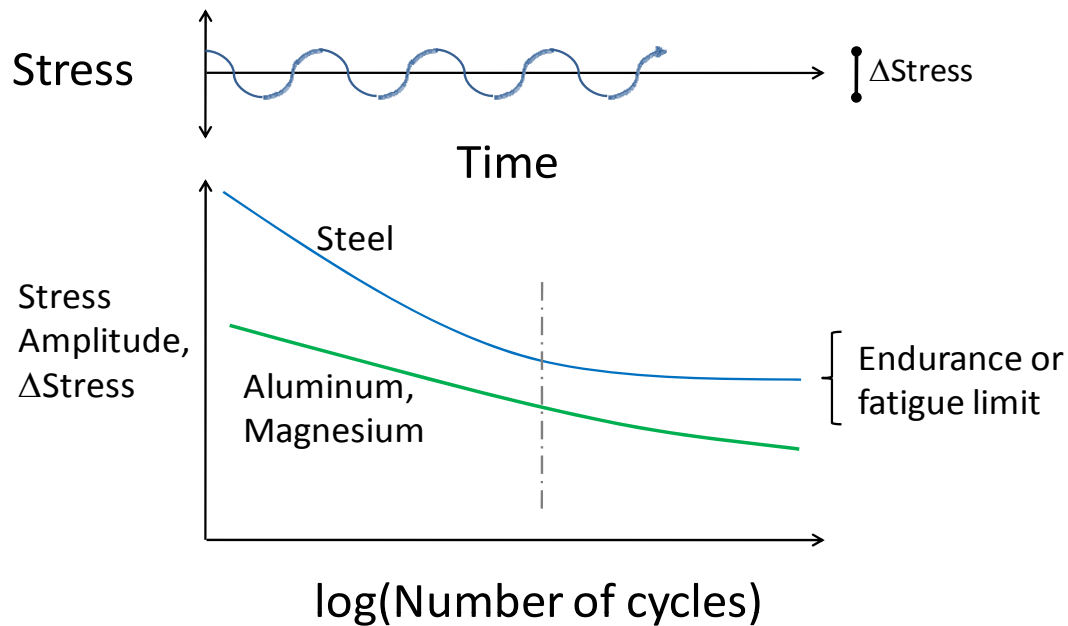
Li-extraction/insertion. The formation of cracks will lead to increased polarization of electrode and poor electric contact between active particles and conductive additives or aluminum foil current collector. This should be one of the



Wöhler *S-N* curve

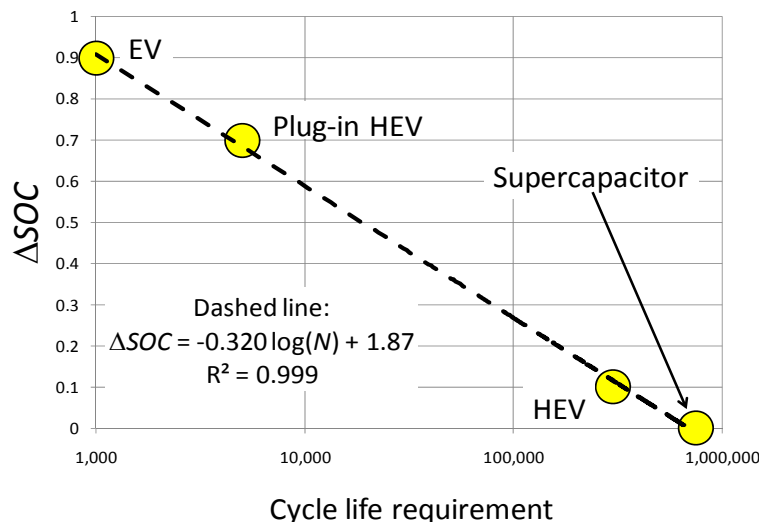
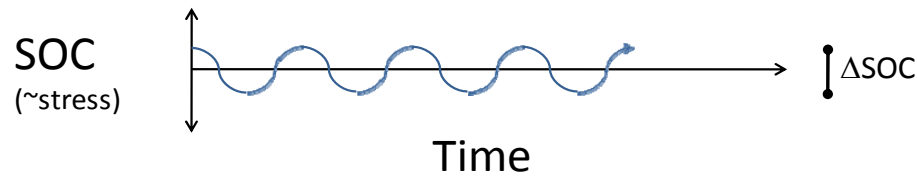
(1870...railroad axles)





□ Direct analogy to the lower cycle-life fatigue... stress amplitude is replaced by ΔSOC

- Temperature & chemical degradation



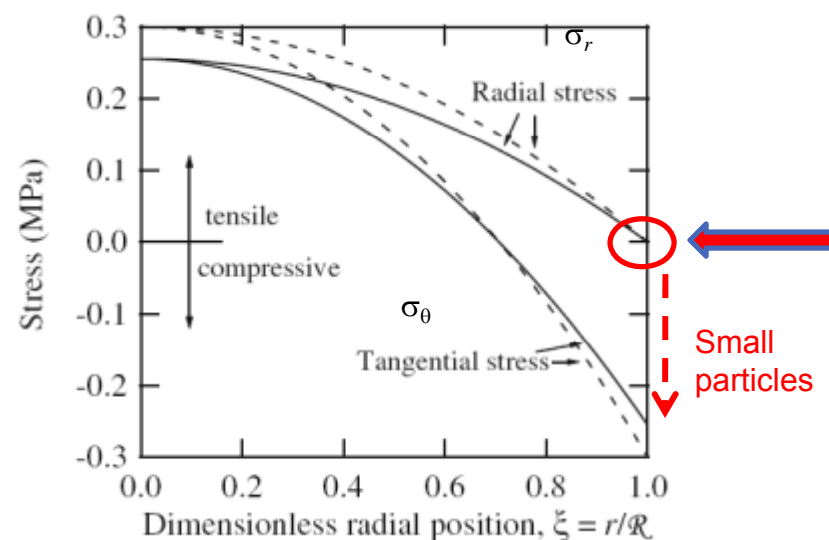
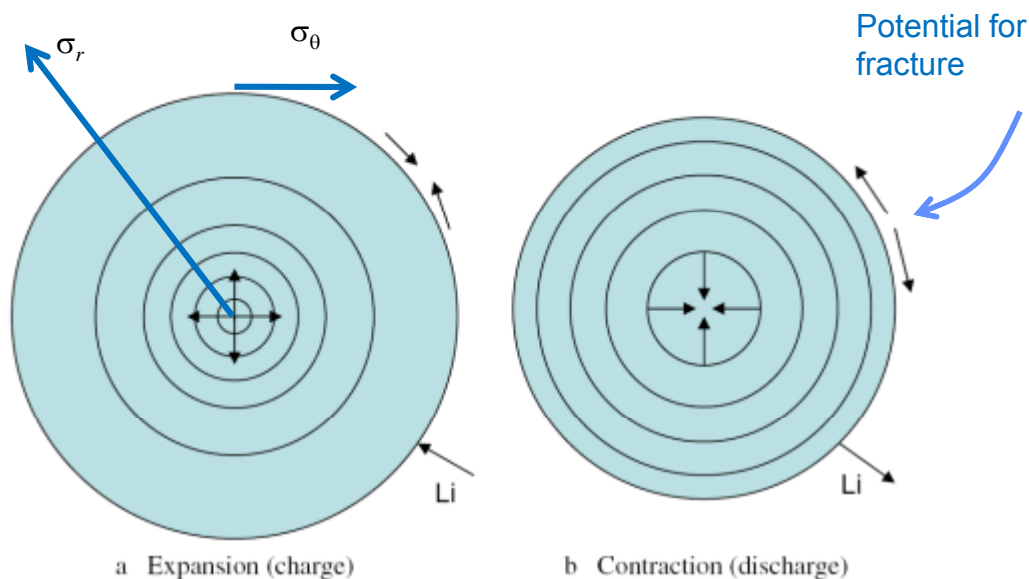
3

□ Model result (next slide): maximum stress is proportional to the maximum difference in SOC, or ΔSOC

□ What about self-healing (“steel-like”) electrodes?

John Christensen · John Newman

Stress generation and fracture in lithium insertion materials



A mathematical model that calculates volume expansion and contraction and concentration and stress profiles during lithium insertion into and extraction from a spherical particle of electrode material has been developed.

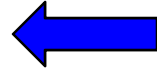
Fig. 5 Simulated normal stress profiles in the particle, as a function of dimensionless radial position, at the end of lithium insertion. Positive values indicate tensile stresses, while negative values correspond to compression. The *solid curves* include the effect of pressure-driven diffusion, while the *dashed curves* neglect it. The parameters used in the simulation are listed in Table 1.



Surface Mechanics. $\sigma_{\theta}^{surf} \equiv \sigma_{\theta\theta}^{surf} = \sigma_{\phi\phi}^{surf} = \tau^0 + K^s \varepsilon_{\theta}$,

where K^s is known as the “surface modulus.” For mechanical equilibrium,

$$\sigma_r(r \rightarrow R) = -\frac{2\sigma_{\theta}^{surf}}{R}$$



NEW for insertion electrode modeling
(Conventional condition recovered for large radius R)

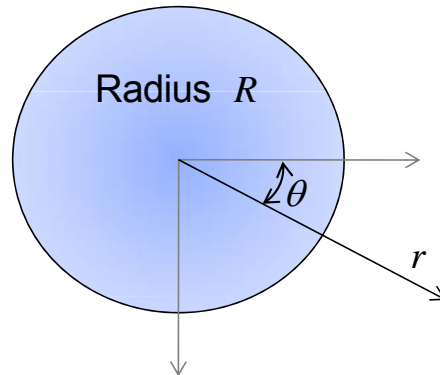
Solid Mechanics

$$\varepsilon_r = \frac{1}{E}(\sigma_r - 2\nu\sigma_{\theta}) + \frac{1}{3}\Omega C$$

$$\varepsilon_{\theta} = \frac{1}{E}[(1-\nu)\sigma_{\theta} - \nu\sigma_r] + \frac{1}{3}\Omega C$$

$$\varepsilon_r = \frac{du}{dr} \quad \text{and} \quad \varepsilon_{\theta} = \frac{u}{r}$$

$$\frac{d\sigma_r}{dr} + 2\frac{\sigma_r - \sigma_{\theta}}{r} = 0$$



Intercalate (lithium) transport

$$\tau = \frac{Dt}{R^2}, \quad x = \frac{r}{R}, \quad \text{and} \quad y = \frac{C(t,r) - C_0}{C_R - C_0} = \frac{\Theta(t,r) - \Theta_0}{\Theta_R - \Theta_0}$$

$$\frac{\partial y}{\partial \tau} = \frac{\partial^2 y}{\partial x^2} + \frac{2}{x} \frac{\partial y}{\partial x}$$

$$y(0, x) = 0$$

$$y(t, 1) = 1$$

$$\frac{\partial y}{\partial x} \Big|_{x=0} = 0$$

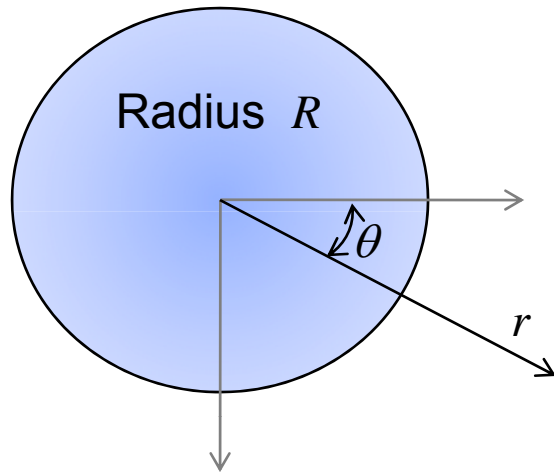
$$\frac{d^2 u}{dr^2} + \frac{2}{r} \frac{du}{dr} - \frac{2u}{r^2} = \left(\frac{1+\nu}{1-\nu} \right) \frac{\Omega}{3} \frac{dC}{dr}$$

$$u(0) = 0$$

This equation system can be solved analytically.

Mathematical details

Potential step, $\Theta_0 \rightarrow \Theta_R$



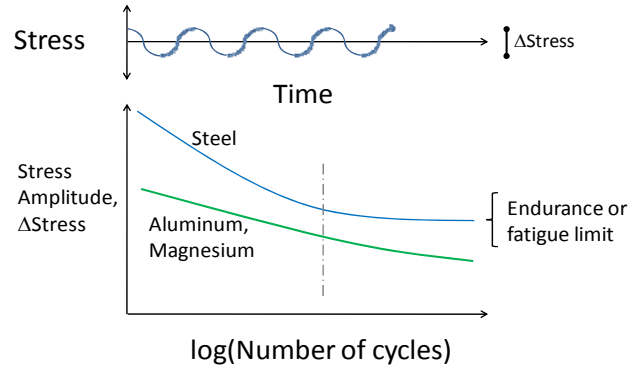
$$\frac{3(1-\nu)}{E\Omega C_s} \sigma_r(t, r) = \frac{2}{3} \Theta_R (S_1 - 1)$$

$$-4(\Theta_R - \Theta_0) \sum_{n=1}^{\infty} \left[\frac{S_1}{(n\pi)^2} + (-1)^n \frac{\sin(n\pi x) - n\pi x \cos(n\pi x)}{(n\pi x)^3} \right] e^{-n^2 \pi^2 \tau} + \frac{3(1-\nu)}{E\Omega C_s} S_2$$

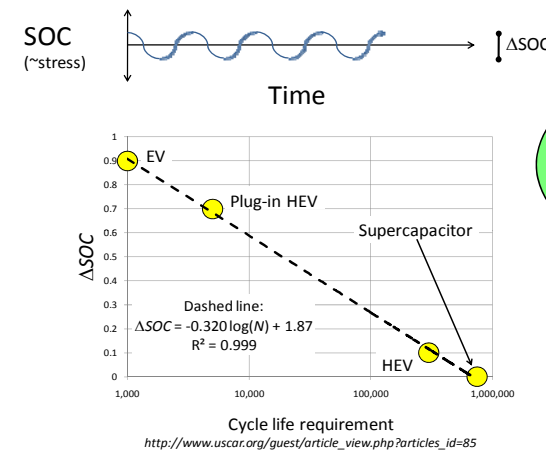
$$\frac{3(1-\nu)}{E\Omega C_s} \sigma_\theta(t, r) = \frac{2}{3} \Theta_R (S_1 - 1)$$

$$-2(\Theta_R - \Theta_0) \sum_{n=1}^{\infty} e^{-n^2 \pi^2 \tau} \left[\frac{2S_1}{(n\pi)^2} - (-1)^n \frac{(\sin n\pi x - n\pi x \cos n\pi x)}{(n\pi x)^3} + (-1)^n \frac{\sin(n\pi x)}{n\pi x} \right] + \frac{3(1-\nu)}{E\Omega C_s} S_2$$

□ For the stress functions, the transient terms are proportional to ΔSOC ($\Delta\text{SOC} \propto \text{stress}$)



- Direct analogy to the lower cycle-life fatigue... stress amplitude is replaced by ΔSOC
 - Temperature & chemical degradation

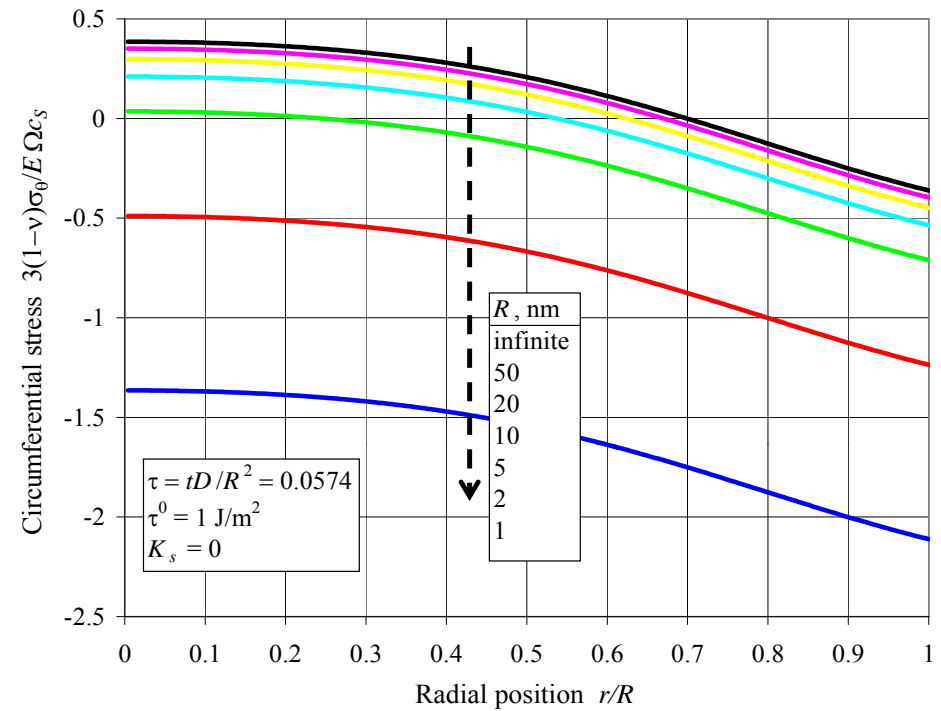
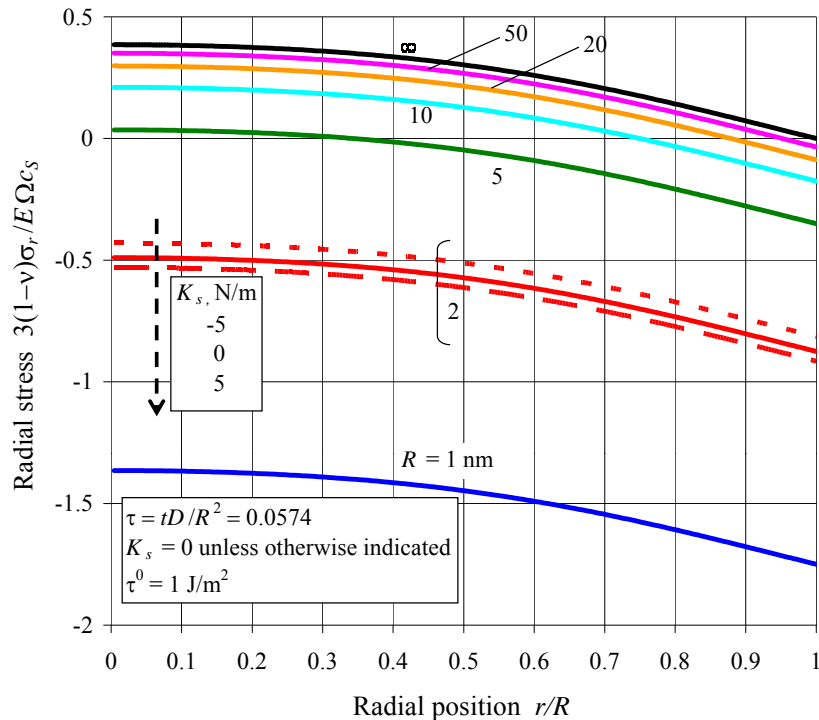


3

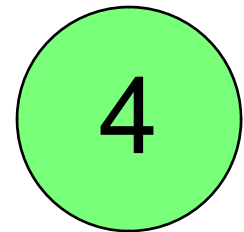
- Model result (next slide): maximum stress is proportional to the maximum difference in SOC, or ΔSOC
- What about self-healing (“steel-like”) electrodes?



Surface Mechanics. $\sigma_{\theta}^{surf} \equiv \sigma_{\theta\theta}^{surf} = \sigma_{\phi\phi}^{surf} = \tau^0 + K^s \varepsilon_{\theta}$ $\sigma_r(r \rightarrow R) = -\frac{2\sigma_{\theta}^{surf}}{R}$



- ❑ Charge (lithiation) of negative (carbon) electrode
- ❑ Influence of surface mechanics is quite significant
 - Radial stress transformed from tensile to compressive
 - Similar influence on tangential (circumferential) stress
- ❑ Note: it is more challenging to make electrodes with smaller particles...enhanced stability comes with a cost

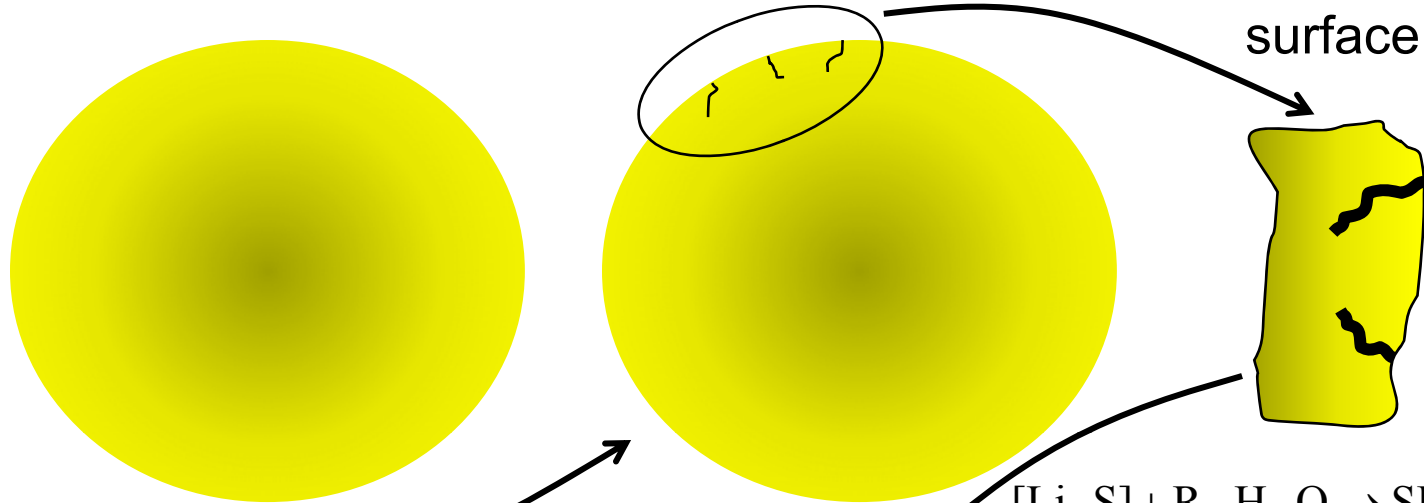




What's wrong with cracks?

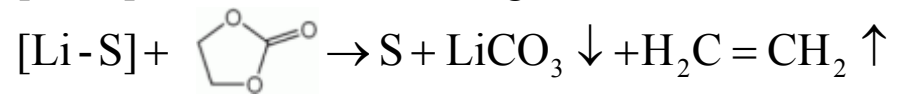
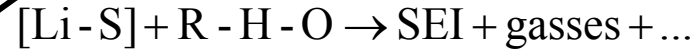
Overall qualitative degradation model...(1) SEI focused

Expanded view of surface



SEI forms on newly exposed surfaces (cracks)

Cracks via cycling



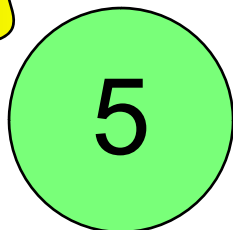
2. Electrode isolation and loss of active material when cracks join

No firm experimental confirmation to date, but consistent with observations

Increased disorder. d_{002} peak-width at half max amplitude increases with time for lithiated carbon

1. Loss of Li: SEI formation and loss of Li seen in full cell experiments

HRL project for observations





Next steps & open questions on life modeling

□ Crack initiation and propagation within a particle

- A difficult problem even in the absence of electrochemical phenomena
- (Griffith) Flaw distributions within electrode particles?
- Primary particles, potentially with grains, and secondary particles (agglomerates)
- Incorporate the influence of chemical degradation processes
- How does temperature come into play?
 - Mechanical deformation of particles is not likely to be affected appreciably by the limited temperature fluctuations
 - Chemical reactions rates are substantially thermally activated

□ Scale up from individual particles to porous electrodes

- Comprehend influence of particle geometry as well as temperature and SOC on physicochemical parameters

□ Construct relevant accelerated life tests



*Looking forward: nano-structures
for improved performance with
lower cost materials*

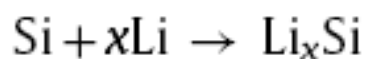


Geometric and electronic studies of $\text{Li}_{15}\text{Si}_4$ for silicon anode

Yu Hong Xu, Ge Ping Yin*, Peng Jian Zuo

Department of Applied Chemistry, Harbin Institute of Technology, 92 West Da-Zhi Street, Harbin 150001, China

For the reaction of Li/Si electrochemical cell:



$V(x)$ can be obtained by following formula:

$$V(x) = - \frac{E_{\text{total}}(\text{Li}_x\text{Si}) - E_{\text{total}}(\text{Si}) - xE_{\text{total}}(\text{Li})}{x}$$

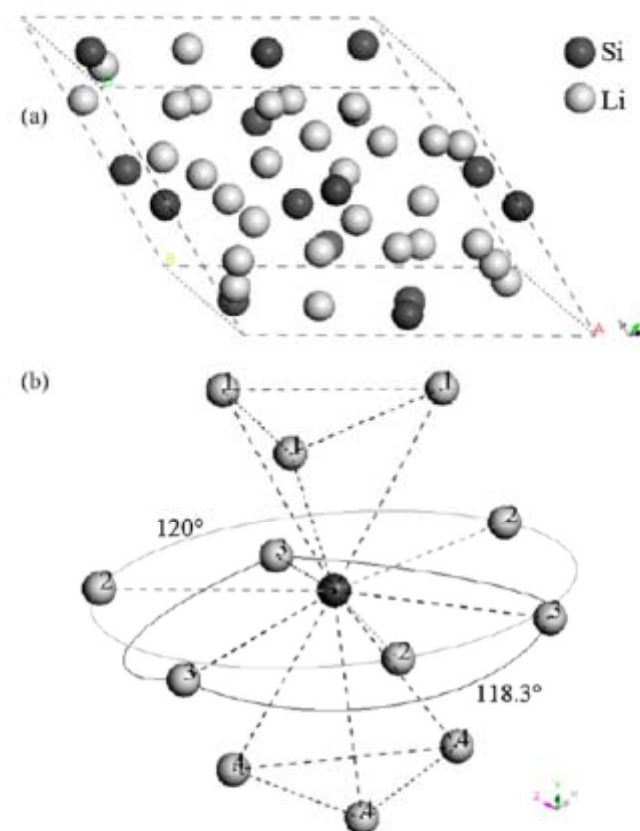


Fig. 1. (a) Primitive cell of $\text{Li}_{15}\text{Si}_4$ and (b) atomic configuration around a Si atom. The Li atoms labeled with the same number indicate same distance with Si atom.

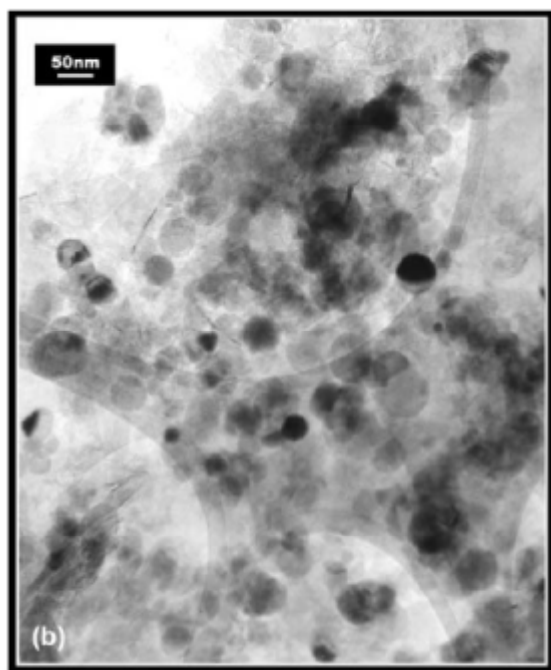
Nanostructured Si–C composite anodes for lithium-ion batteries

G.X. Wang^{*}, J.H. Ahn, Jane Yao, Steve Bewlay, H.K. Liu

Institute for Superconducting and Electronic Materials, University of Wollongong, Wollongong, NSW 2522, Australia

Received 19 April 2004; accepted 11 May 2004

Available online 2 June 2004



(b) TEM image of nanocrystalline Si–C composites.

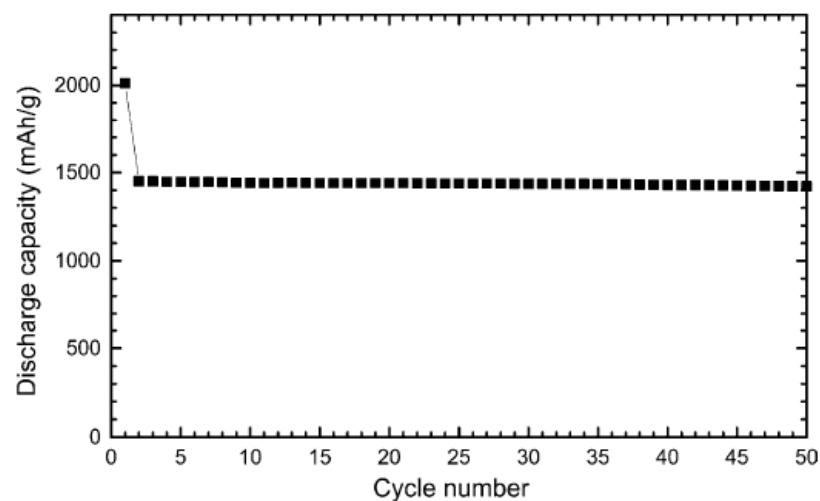


Fig. 3(b) shows a TEM photo of nano Si–C composite powders. It clearly demonstrates that Si powders are surrounded by amorphous carbon. Spot EDX (energy dispersive Xray) analysis confirmed that the spherical black crystals in Fig. 3(b) are Si. Therefore, nanocrystalline Si particles are uniformly embedded in amorphous carbon matrix through the carbon aerogel synthesis process.



Li₂MnO₃-stabilized LiMO₂ (M = Mn, Ni, Co) electrodes for lithium-ion batteries†

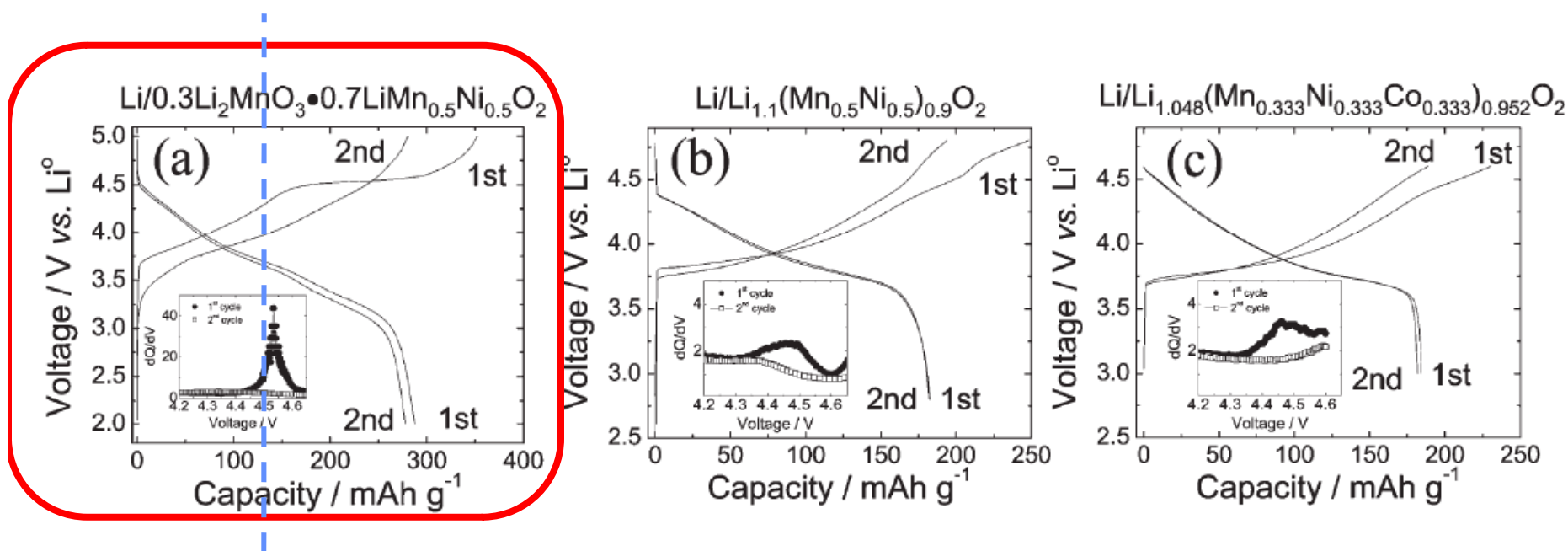
Michael M. Thackeray,^{*a} Sun-Ho Kang,^a Christopher S. Johnson,^a John T. Vaughey,^a Roy Benedek^a and S. A. Hackney^b

Received 16th February 2007, Accepted 29th March 2007

First published as an Advance Article on the web 20th April 2007

DOI: 10.1039/b702425h

A strategy used to design high capacity (>200 mAh g⁻¹), Li₂MnO₃-stabilized LiMO₂ (M = Mn, Ni, Co) electrodes for lithium-ion batteries is discussed. The advantages of the Li₂MnO₃ component and its influence on the structural stability and electrochemical properties of these layered xLi₂MnO₃·(1 - x)LiMO₂ electrodes are highlighted. Structural, chemical, electrochemical and thermal properties of xLi₂MnO₃·(1 - x)LiMO₂ electrodes are considered in the context of other commercially exploited electrode systems, such as LiCoO₂, LiNi_{0.8}Co_{0.15}Al_{0.05}O₂, Li_{1+x}Mn_{2-x}O₄ and LiFePO₄.





Summary

1. Recognize the importance of the SEI/protective layers

2. Calendar life

- Large particles are desired for low surface area (and lower cost manufacturing)

3. Cycle life

- Small particles are desired to reduce mechanical deformation and surface cracking (and reduce transport & charge-transfer resistance)

□ Life is a balancing act